

T-4119

GENESIS OF RED SANDSTONES ASSOCIATED WITH VANADIUM-URANIUM
DEPOSITS IN THE SALT WASH MEMBER OF THE MORRISON
FORMATION, SLICK ROCK DISTRICT,
SAN MIGUEL COUNTY, COLORADO

by
Phillip J. Allen

ARTHUR LAKES LIBRARY
COLORADO SCHOOL OF MINES
GOLDEN, CO 80401

ProQuest Number: 10783765

All rights reserved

INFORMATION TO ALL USERS

The quality of this reproduction is dependent upon the quality of the copy submitted.

In the unlikely event that the author did not send a complete manuscript and there are missing pages, these will be noted. Also, if material had to be removed, a note will indicate the deletion.



ProQuest 10783765

Published by ProQuest LLC (2018). Copyright of the Dissertation is held by the Author.

All rights reserved.

This work is protected against unauthorized copying under Title 17, United States Code
Microform Edition © ProQuest LLC.

ProQuest LLC.
789 East Eisenhower Parkway
P.O. Box 1346
Ann Arbor, MI 48106 – 1346

T-4119

A thesis submitted to the Faculty and Board of Trustees of the Colorado School of Mines in partial fulfillment of the requirements for the degree of Master of Science (Geochemistry).

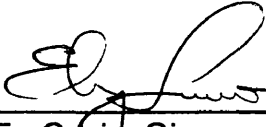
Golden, Colorado

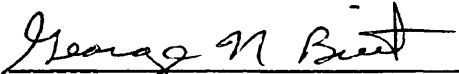
Date 4-10-92

Signed:


Phillip J. Allen


Approved:


E. Craig Simmons
Thesis Co-advisor


George N. Breit
Thesis Co-advisor

Golden, Colorado

Date 4/10/92


Stephen R. Daniel, Head
Department of Chemistry
and Geochemistry

Abstract

Epigenetic vanadium-uranium deposits in southwestern Colorado and southeastern Utah are hosted in fluvial sandstones of the Salt Wash Member of the Upper Jurassic Morrison Formation. These deposits are entirely within gray-green sandstones. However, large ore deposits are common near red sandstones, which has lead exploration geologists to propose a genetic relation between the red sandstone and vanadium-uranium ore deposits. The purpose of this study is to gain a better understanding of these red sandstones and their possible relation to high grade ore deposits. Samples were collected in the Sunday Mine, Slick Rock district Colorado, that represent the gray-green, red, and transitional sandstone. Additional samples were collected from the Deremo Mine, outcrops on Horse Range Mesa, and a core that is 600 meters from any known vanadium-uranium deposit. Petrographic data were collected using transmitted light and obliquely reflected light microscopy, and a scanning electron microscope. The relative abundance and alteration textures were recorded for hematite, pyrite, magnetite, ilmenite, leucoxene, native sulfur, quartz, chert, chalcedony, calcite, gypsum, and pore-filling clay.

The sandstone samples reveal three distinct diagenetic stages associated with the reddening of the Salt Wash Member channel sandstones. The first stage, shallow burial I, was active in the

vicinity of detrital organic matter. Pore waters in these sandstones were reducing because of organic matter and bacterial H_2S . The reducing conditions caused pyrite precipitation and altered detrital magnetites and ilmenites by leaching iron and forming leucoxene. Second, during the shallow burial II stage a weakly alkaline oxygenated meteoric water was introduced into portions of the reduced channel sandstone. This solution partially dissolved pyrite, precipitated hematite, and preserved detrital magnetites and ilmenites. The third and final stage of alteration occurred during deep burial after inflow of oxygenated meteoric water ceased and the reducing conditions encroached into the oxidized sandstone. This deep burial stage reduction partially dissolved hematite while precipitating pyrite, native sulfur, and microcrystalline TiO_2 .

The oxygenated meteoric water from the second event is inferred to have been the transport medium for the ore metals based upon the timing of the vanadium-uranium accumulation. This solution transported uranium leached from volcanic ash in the Brushy Basin Member. The vanadium-uranium deposits in the Uravan mineral belt are not found on the boundary between red and gray-green sandstone, like the Wyoming roll front deposits, because of deep burial reduction and bleaching of the oxidized red sandstone. It is concluded that following the red gray-green sandstone boundary is a valid method of exploration for some vanadium-uranium deposits.

T-4119

However, reduction during deep burial may have moved the boundary substantially away from the present ore bodies.

TABLE OF CONTENTS

	Page
ABSTRACT	iii
LIST OF FIGURES	vii
LIST OF TABLES	x
ACKNOWLEDGEMENTS	xi
INTRODUCTION	1
GEOLOGIC SETTING	9
EXPERIMENTAL	16
FIELD STUDY	16
LABORATORY STUDY	19
RESULTS	22
DISCUSSION	38
SHALLOW BURIAL	40
SHALLOW BURIAL I	41
SHALLOW BURIAL II	43
DEEP BURIAL	49
IMPLICATIONS TO VANADIUM-URANIUM EXPLORATION	54
CONCLUSION	55
REFERENCES CITED	60
APPENDIX	68

LIST OF FIGURES

	Page
Fig. 1: Generalized geologic map of the Slick Rock vanadium-uranium district showing mine and sample locations. (modified from Breit and Meunier, 1990)	2
Fig. 2: Generalized map showing the distribution of ore bodies, upper reduced channel sandstone, and oxidized flood plain mudstones of the Salt Wash Member, La Sal Channel, San Juan County, Utah (modified from Thamm et al., 1981).	5
Fig. 3: Schematic cross section of a boundary between gray and red sandstone entirely within sandstone, Deremo Mine (modified from Thamm et al., 1981)	6
Fig. 4: Plan view of the Sunday Mine workings and enlargement of stope 1882, showing distribution of known red sandstone.....	17
Fig. 5: Map of the south rib of drift leading to stope 1882, Sunday Mine, and graphs showing the relative concentrations of key phases across the drift.	18
Fig. 6: Plan view of the Deremo Mine, showing distribution of known red sandstone and sample locations (modified from Thamm et al., 1981).....	20
Fig. 7: Map of the northeast rib showing sample locations, located in Figure 6, Deremo Mine.	21

Fig. 8: Photomicrograph in oblique reflected light of pore-filling clay coated with amorphous pigmentary hematite (H) and surrounded by detrital quartz grains (Q). Hematite has been removed from edges of pore-filling clay. Field of view = 1.0 mm wide. 25

Fig. 9: Photomicrograph in transmitted plane polarized light of void space filled with blue epoxy between detrital quartz grain (Q) and quartz overgrowth (og). Field of view = 0.2 mm wide. 25

Fig.10: Photomicrograph in transmitted plane polarized light of hematite (H) within quartz overgrowths (og) and between overgrowths and calcite (C). Field of view = 0.5 mm wide.. . . . 26

Fig. 11: Photomicrograph in oblique reflected light of hematite (H) coating authigenic leucoxene (L). (detrital quartz grain (Q)). Field of view = 0.2 mm wide. 26

Fig. 12: Photomicrograph in transmitted plain polarized light of detrital grain stained with hematite (H) subsequently relaced by quartz (q) and carbonate (c) cement. (detrital quartz grain (Q)). Field of view = 0.5 mm wide. 27

Fig. 13: Photomicrograph in oblique reflected light of hematized detrital magnetite grain (Hm), hematite within quartz overgrowth (H) and detrital quartz grains (Q). Field of view = 0.2 mm wide. 27

Fig. 14:	SEM micrograph of hematite crystals (H) within illite (I).....	29
Fig. 15:	SEM micrograph of aggregates of hematite crystals (H) with quartz (Q) and authigenic chlorite (CHL).	29
Fig. 16:	Photomicrograph in oblique reflected light of authigenic subhedral pyrite (P) with reaction rim (r), surrounded by detrital quartz grains (Q). Field of view = 0.5 mm wide.....	30
Fig. 17:	SEM micrograph of pyrite cubes (P) that are partially dissolved on top and bottom faces.....	30
Fig. 18:	SEM micrograph of pyrite (P) with a platy morphology.....	32
Fig. 19:	Photomicrograph in oblique reflected light of detrital magnetite (M) partially altered to hematite (H) and leucoxene (L). Surrounded by detrital quartz grains (Q). Field of view = 0.2 mm wide..	32
Fig. 20:	SEM micrograph of detrital titanomagnetite grain (tM).	33
Fig. 21:	Photomicrograph in oblique reflected light of authigenic spherical leucoxene grain (L), partially altered angular detrital magnetite grain (M), and detrital quartz grains (Q). Field of view = 0.5 mm wide..	33
Fig. 22:	Photomicrograph in oblique reflected light of angular authigenic leucoxene grain (L), surrounded by quartz cement (q), and	

detrital quartz grains (Q). Field of view =
0.5 mm wide.. 34

Fig. 23: Photomicrograph in oblique reflected light
of partially dissolved detrital feldspar
grain with inclusions of leucoxene (L) and
detrital quartz grains (Q). Field of view =
0.5 mm wide.. 34

Fig. 24: SEM micrograph of leucoxene grain
aggregate (L) surrounded by chlorite (CHL). 35

Fig. 25: SEM micrograph of microcrystalline
leucoxene between detrital quartz grain (Q)
and quartz overgrowth (og), and partially
dissolved K-feldspar (K). 37

Fig. 26a: Diagram summarizing the Shallow Burial I
Stage with a portion of the channel
sandstone remaining reduced due to
dissolved organic material and bacterial
activity. Channel sandstone is approximatly
100 m wide. 56

Fig. 26b: Shallow Burial II Stage. Oxygenated
meteoric water from the Brushy Basin
Member and the Salt Wash Member overbank
mudstones entered reduced sandstones. The
meteoric water carried vanadium and
uranium. Dissolved oxygen was depleted
from iron (II) oxidation. Ore metals
precipitated because of reduction during
reaction with dissolved organic matter and
H₂S. 57

Fig. 26c: Diagram summarizing the Deep Burial Stage.
Arrows show the bleaching of reddened
sandstone after flux of oxidizing fluid from

the Brushy Basin Member stops, by dissolved
organic matter and bacterial activity from
reduced sandstone. 58

LIST OF TABLES

Table	Page
1. Generalized stratigraphy of the sedimentary rocks in the Slick Rock district (modified from Breit and Meunier, 1990).	10
2. Paragenetic sequence of authigenic phases in the Salt Wash Member of the Morrison Formation associated with oxidation in the Slick Rock district.	39
3. Parameters for the calculation of time needed for the generation of the Deremo Mine.	47

ACKNOWLEDGEMENTS

The author would like to acknowledge Dr. George Breit and Mr. Stu Hollingsworth for their guidance and patience during the course of this project. Dr. E. Craig Simmons was most helpful with his unbiased perspective of these deposits. The discussions between the author and Dr. Maynard Slaughter about the Slick Rock and Wyoming type vanadium-uranium deposits were very insightful. Also the help of friends and fellow graduate students in the Chemistry and Geochemistry and Geology Departments was needed more than once throughout this project.

This project was funded by the Umetco Mineral Corporation's exploration and mining departments. The support and assistance of the staff and miners at the La Sal, the Sunday, and the Deremo mines added many insights to the understanding of vanadium-uranium deposits.

The financial and moral support of my family, especially mom and dad, was tremendous and without it, this thesis would not have been completed. Finally, I thank the one individual who is responsible not only for this thesis but my entire career, Fred H. Crone. Without my introduction and instilled passion for mineralogy from him, none of this would ever have been possible. May I carry his creativity and optimism through the rest of my travels.

INTRODUCTION

Fluvial sandstones of the Salt Wash Member of the Upper Jurassic Morrison Formation host vanadium-uranium deposits in southwestern Colorado and southeastern Utah. Fischer and Hilpert (1952) found that many of the largest, highest grade, and closest spaced of these deposits are arranged in a narrow arc-shaped belt trending north-south and named it the Uravan mineral belt (Figure 1). The Uravan mineral belt vanadium-uranium deposits are epigenetic, tabular and roll-shaped bodies. Unlike the Wyoming and Texas roll front deposits, where ore is found mainly between red and white sandstones, the Uravan deposits are entirely within gray-green sandstone (Shawe 1976).

Many genetic models, syngenetic and epigenetic, have been proposed to explain vanadium-uranium deposits (Adams, 1991). Because the deposits are not confined by primary sedimentary structures, such as cross bedding, syngenetic models have been discarded. Shawe (1976) proposed that compaction of the Cretaceous Mancos Shale drove uranium-bearing water down along faults into the Salt Wash Member and ore precipitated in the vicinity of carbonaceous material. The lacustrine-humate model (Peterson and Turner-Peterson, 1980) proposed that humic acids which were expelled from lake beds into sandstones formed a tabular layer that accumulated vanadium and uranium carried by ground water. Granger

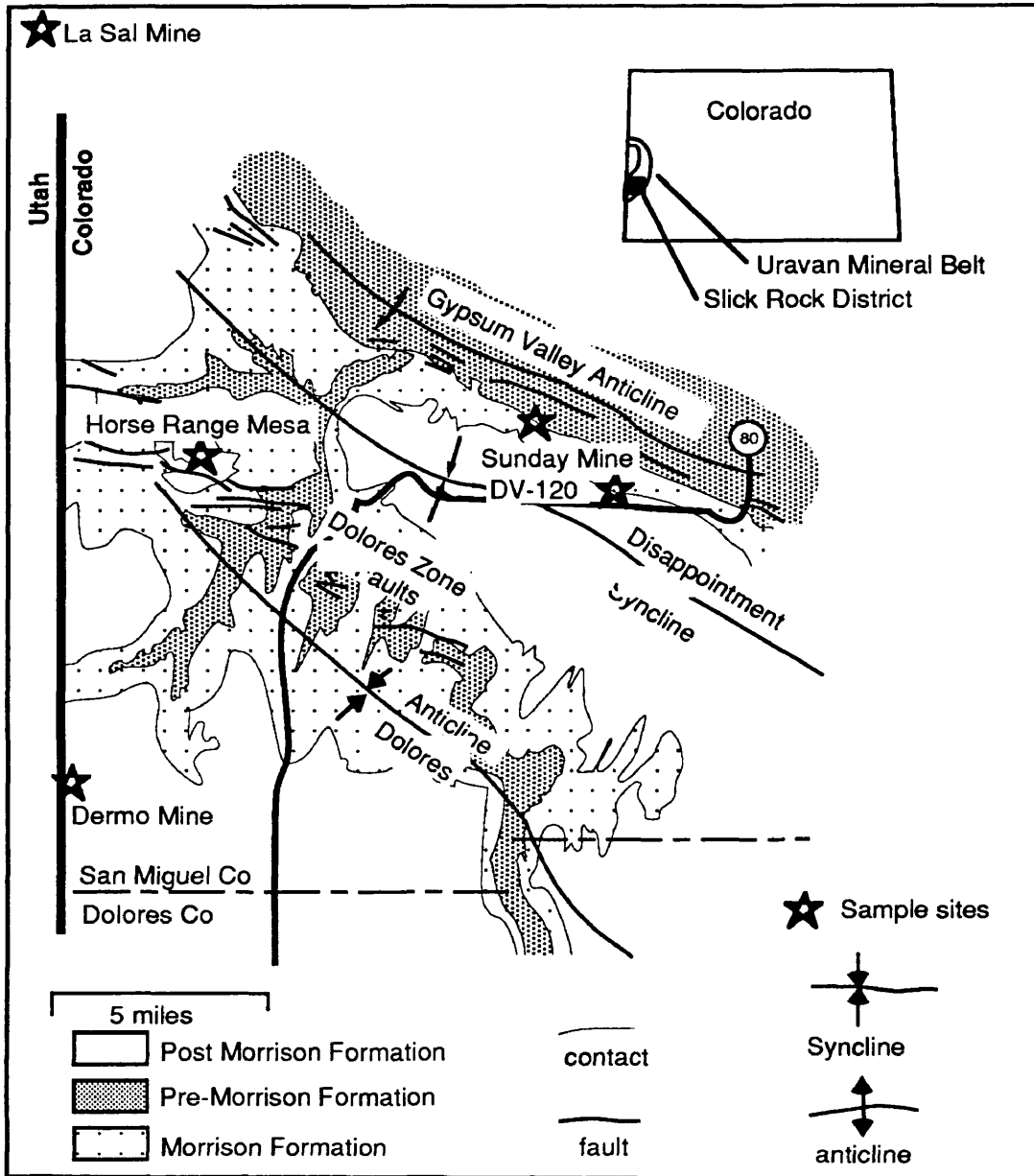


Figure 1: Generalized geologic map of the Slick Rock vanadium-uranium district showing mine and sample locations. (modified from Breit and Meunier, 1990)

and Warren (1981) suggested that ore formed because two ground waters mixed, one contained organic ligands and vanadium(III) and the other contained uranium(VI). In their model, vanadium(III) reduced uranium(VI) to the less soluble uranium(IV) which caused uranium and vanadium oxides to precipitate. Because the vanadium-uranium deposits are commonly associated with chrome-rich clays and iron deposits, Breit and Goldhaber (1989) proposed that ore deposition occurred at the interface of an oxygenated alkaline pore water carrying ore metals and a reducing sulfidic pore water. Northrop (1982) and Northrop et al. (1990) found systematic changes in the oxygen, hydrogen, and carbon isotopic composition of clays and carbonate minerals below and within ore in the Henry Basin and attributed these trends to meteoric water mixing with a lower basin brine. The current epigenetic models subscribe to the theory that ore deposition occurred at the interface of two different fluids. An additional process commonly associated with the two fluid interface is the roll-front model. The roll-front model suggests that after initial precipitation, the ore was remobilized and reprecipitated farther down the hydrologic gradient. Remobilization of ore is commonly referred in the literature to explain the Wyoming and Texas uranium deposits and redistribution of ore in the Grant's uranium region, New Mexico (Adler, 1974)

In the Uravan mineral belt red sandstone is sporadically found next to high grade vanadium-uranium ore, and the highest grade ore

is commonly found where red rock intertongues with gray sandstone (Nestler and Chenoweth, 1958; Thamm et al., 1981). Since vanadium and uranium are soluble and mobile in high pH oxygenated fluids (Langmuir, 1978) and the hematite in red sandstone is consistent with oxidation, the red sandstone may reflect an important condition of ore formation. The spatial association has led many exploration geologists to follow along a red-white sandstone boundary in the Salt Wash Member as a method of locating new vanadium-uranium deposits. However the empirical relationships have defied interpretation due to a lack of understanding of the formation of both the vanadium-uranium deposits and the red sandstone.

Thamm et al. (1981) identified two types of boundaries between red and white rocks in the Salt Wash Member. The first is the contact of dominantly white channel sandstone with dominantly red overbank and floodplain mudstone. For example in the La Sal Mine, Utah (Figures 1 and 2) ore is found along the south side of a east-west trending gray-green channel sandstone that is bounded by red mudstones. The second type of red-white boundary is a gradational change of gray-green to red channel sandstone as is found in the Deremo Mine (Figures 1 and 3). Evaluating this second type of contact is the focus of this study.

The contrast in color between red and gray-green sandstones is largely due to differences in the abundance and type of Fe-rich minerals. The iron phases that affect the color of the rock are

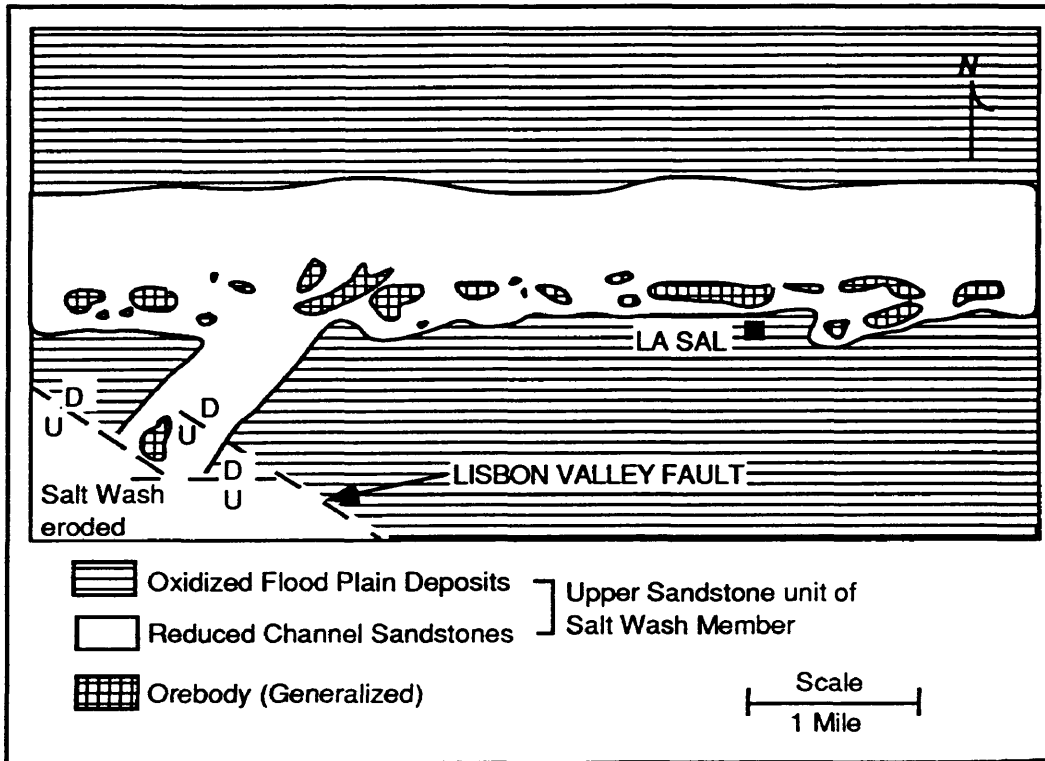


Figure 2: Generalized map showing the distribution of ore bodies, upper reduced channel sandstone, and oxidized flood plain mudstones of the Salt Wash Member, La Sal Channel, San Juan County, Utah (modified from Thamm et al., 1981).

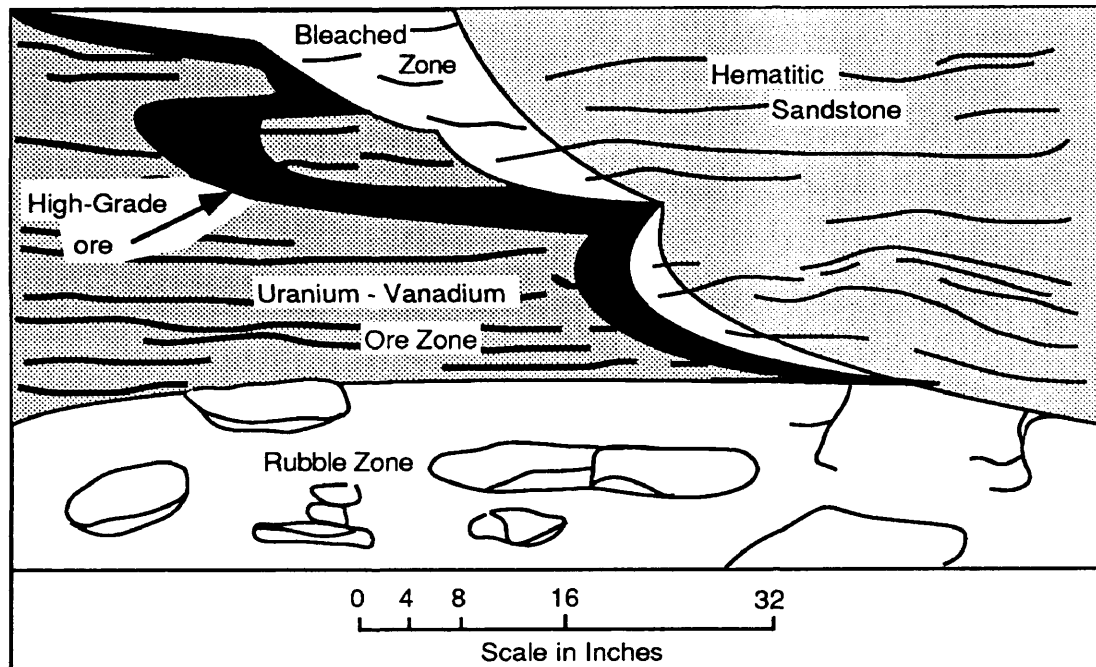


Figure 3: Schematic cross section of a boundary between gray and red sandstone entirely within sandstone, Deremo Mine (modified from Thamm et al., 1981)

hematite, goethite, ferrihydrite, lepidocrocite, and clay minerals. Hematite can color the rock from a purplish red to yellowish red depending upon the particle size and the clustering of hematite particles (Torrent and Schwertmann, 1986). The iron oxyhydroxides, goethite, ferrihydrite, and lepidocrocite, produce a yellowish to a brownish color to the rock (Pye, 1983). Iron-rich clays typically produce a greenish color. Other minor iron phases, such as pyrite and magnetite, do not produce a significant color change to the rock.

The iron minerals reflect the oxidation state of iron and the redox history of the rock. Iron in nature has two oxidation states (III) and (II). Common iron (III) minerals are hematite, goethite, ferrihydrite, and lepidocrocite. The iron oxyhydroxides typically precipitate from the oxidation of iron such as hematite, form by the dehydration and recrystallization of iron oxyhydroxides (Pye, 1983). Iron-rich clay minerals can contain iron (II) or (III) and form under a variety of conditions (Stumm and Morgan, 1981). Pyrite contains iron (II) and in sedimentary rocks typically forms in low temperature, reducing, sulfidic conditions. Magnetite contains both iron (II) and (III), and is most commonly a high temperature and pressure mineral but has been formed bacteria (Frankel and Blakemore, 1984). Careful study of the iron-rich minerals can therefore be used to evaluate the composition of fluids that moved through the rocks.

Shawe (1976) identified three diagenetically altered facies based on the distribution of the iron-rich phases in Salt Wash Member sandstones in the Slick Rock district. They include (1) red bed, (2) carbon and (3) altered. Red-bed facies are light reddish brown with abundant detrital black opaque heavy minerals (mainly magnetite and ilmenite), hematite films that coat detrital grains, and dustlike inclusions of hematite dispersed within matrix material. The carbon-facies is a light gray or greenish gray and contains detrital carbonized plant fragments, moderate amounts of black heavy minerals, a small amount of pyrite, and no pigmentary hematite. The altered-facies rocks which host the vanadium-uranium deposits, are light gray or greenish gray, have sparse black opaque heavy minerals, significant pyrite, no hematite, and may or may not contain carbonaceous material. Altered-facies rocks are common in permeable sandstones, and selvages of argillaceous rocks in the vicinity of fractures. Alteration affected both red-bed and carbon facies resulting in loss of black opaque minerals. In addition pigmentary iron oxides were dissolved from red beds. In a similar study, Adams et al. (1974) studied the Morrison Formation in the San Juan Basin and noted that magnetites and ilmenites were also altered by dissolution near uranium deposits.

The purpose of this study is to better understand the formation of red sandstone near vanadium-uranium ore and to determine if there is a genetic relationship between the two. The iron and iron

related minerals, such as pyrite, leucoxene, ilmenite and magnetite, were examined in red and gray to greenish gray channel sandstones near ore in the Salt Wash Member. In addition, the composition and diagenetic history of red sandstones was examined to identify any difference between red sandstone near ore and red sandstone distant from ore. The authigenic minerals were then placed into a paragenetic sequence that reflects changes in pore water chemistry. The composition of the pore waters was estimated from the authigenic minerals and the alteration associated with them. The stability of the red to gray-green channel sandstone boundary was also evaluated. The final question addressed was whether the red-white boundary is a suitable exploration tool.

GEOLOGIC SETTING

The areas studied for this investigation are within the Slick Rock vanadium-uranium district in southwestern Colorado (Figure 1). The district covers 570 square miles and is located in western San Miguel and Dolores counties. The exposed sedimentary rocks in the Slick Rock district are 4,700 feet thick and range from Permian to Cretaceous (Table 1) (Shawe, 1976). Sedimentary rocks as old as Devonian are in the subsurface. The district is at the southeast end of the Paradox fold and fault belt. Diapiric uplift and collapse since the Permian, of bedded evaporites of the Paradox Member of the

Table 1: Generalized stratigraphy of the sedimentary rocks in the Slick Rock district (modified from Breit and Meunier, 1990).

UNIT	THICKNESS(m)	LITHOLOGY
<u>Cretaceous</u>		
Mancos Shale	500 to 750	Carbonaceous, calcareous marine mudstone
Dakota Sandstone	36 to 55	Marine and Fluvial sandstone, carbonaceous shale and coal
Burro Canyon Formation	12 to 120	Fluvial sandstone, green shale
<u>Jurassic</u>		
Morrison Formation		
Brushy Basin Member	90 to 210	Lacustrine mudstone, siltstone, channel sandstone
Salt Wash Member	80 to 120	Fluvial sandstone, flood plain mudstone
Tidwell Member	3 to 10	Flood plain mudstone and siltstone, fluvial sandstone
Wanakah Formaiton	25 to 50	Lacustrine siltstone and fine-grained sandstone
Entrada Sandstone	27 to 46	Eolian and tidal flat sandstone
Navajo Sandstone	0 to 130	Eolian sandstone
Kayenta Formation	52 to 60	Fluvial siltstone and sandstone
Wingate Sandstone	60 to 120	Eolian sandstone
<u>Triassic</u>		
Chinle Formation	100 to 200	Fluvial and lacustrine shale, sandstone, and siltstone
<u>Permian</u>		
Cutler Formation	450 to 920	Fluvial and flood plain sandstone, siltstone, and mudstone
<u>Pennsylvanian</u>		
Rico Formation	40 to 75	Transition between Cutler and Hermosa Formation
Hermosa Formation	1,200 to 2,100	Marine limestone, dolostone, evaporite and black shale

Hermosa Formation produced northwest trending anticlines and synclines (Cater, 1970). Folds within the district include the Disappointment syncline, which is bounded by the Dolores anticline to the southeast and by Gypsum Valley anticline to the northwest. Gypsum Valley anticline was breached due to dissolution of the Pennsylvanian evaporites and subsequent collapse and erosion of sedimentary rocks younger than the evaporites. There are two major fault systems aligned parallel to the anticlines, the Dolores zone of faults and Gypsum Valley faults. The Dolores zone of faults is a band of subparallel faults 3 km wide with a minimum displacement of 3 m. The Gypsum Valley faults include faults formed by collapse following dissolution of evaporites and some fractures have bleached (white) selvages where they cross otherwise red rocks.

The Salt Wash Member of the Late Jurassic Morrison Formation was deposited by broad and deep low-sinuosity streams that deposited dip-elongate bodies of sand (Tyler and Ethridge, 1983). Three distinct sedimentary units in the Salt Wash Member are the laterally continuous lower and upper sandstone units which are separated by an interval of interbedded mudstone and discontinuous sandstone. The average thicknesses of the upper sandstone, interbedded mudstone, and lower sandstone units are 30 m, 70 m and 10 m respectively (Tyler and Ethridge, 1983; unpublished Umetco report). Tyler and Ethridge (1983) interpreted the sandstone architecture of the Slick Rock district as that of a zone of

convergence of smaller streams into a trunk river. The Uravan mineral belt, defined by Fischer and Hilpert (1952), could be related to a larger zone of stream convergence that characterized the midpoint of the paleoslope of the Salt Wash Member.

The Salt Wash Member, in the Slick Rock district, consists of 60 volume percent sandstone, 39 percent siltstone, claystone and mudstone, and 1 percent limestone and conglomerate (Cadigan, 1967). The sandstones are fine grained and moderately sorted. A typical sandstone contains greater than 65 percent detrital monocrystalline quartz with minor orthoclase, clays, plagioclase, devitrified tuff and rock fragments (Cadigan, 1976) and is classified as a subarkosic arenite (Tyler, 1981). Authigenic cements include calcite, quartz, barite, dolomite, iron oxide and gypsum, which are present in variable amounts (Cadigan, 1967; Breit, 1986).

Iron oxide and sulfide minerals in the Salt Wash include hematite, limonite, magnetite, ilmenite, and pyrite (Bowers and Shawe, 1961; Shawe, 1968, 1976; Breit, 1986). Hematite is found as inclusions between quartz grains and overgrowths, dustings dispersed in authigenic matrix material, plates radiating from detrital grains, and round to sub-round detrital grains. Limonite, is found as irregular fragments or pseudomorphs after pyrite, ranges in abundance from trace to three volume percent (Bower and Shawe, 1961) and is only found in Salt Wash Member rocks exposed to surficial weathering. Detrital magnetite and ilmenite grains are a

less than 1 weight percent of the total rock, and range from round to angular. The common round grains are the result of abrasion during fluvial transport while angular grains are interpreted as partially altered detrital grains (Bower and Shawe, 1961) Martite, after magnetite, has been identified but its origin is uncertain. Pyrite is associated with gray-green rocks, coalified plant fragments, and vanadium-uranium deposits, in amounts ranging from trace to 80 volume percent. The morphology of the pyrite is euhedral to subhedral cubes, pyritohedrons, irregular fragments, fine grained crystalline aggregates, and rod shaped fossil replacements.

Authigenic titanium minerals are found in the Salt Wash Member as less than 0.1 weight percent of the total rock. Leucoxene has a spheroidal or irregular shape and ranges from a trace to 42 % of the heavy mineral fractions (Bower and Shawe, 1961). It is mixed with hematite, ilmenite, hematitic laminae, and forms dustlike inclusions within barite. Even though anatase, brookite, pseudobrookite, microcrystalline and amorphous TiO_2 have been identified in the Salt Wash Member, they are commonly grouped together as leucoxene due to the limitations of petrographic identification. Based upon the morphology and relation to other authigenic minerals, leucoxenes are interpreted as authigenic (Adams et al. 1974).

The vanadium-uranium deposits of the Morrison Formation are found in gray-green sandstone, and are commonly associated with

carbonaceous trash. They are tabular and peneconcordant with bedding, but locally define rolls that sharply cross bedding (Shawe, 1956). All major ore deposits in the Slick Rock District are within the uppermost sandstone rim of the Salt Wash Member. Even though ore mineralization was not controlled by primary sedimentary structure, vanadium-uranium minerals are locally concentrated along foresets of cross beds. The occurrence and distribution of ore is sometimes attributed to the types of sandstone packages (Tyler and Ethridge, 1983). Uranium is typically found as uranium (IV) minerals, uraninite and coffinite. Vanadium typically is in a (III) oxidation state in montroseite and in the interlayer octahedral sheet of clays (Whitney and Northrop, 1986).

The ore deposits in the district range from a few meters to a few hundred meters in length and less than one meter to 10 meters in thickness (Thamm et al., 1981). The small mines are much more numerous than larger ones, as seen by the many small mining operations scattered throughout the district (Thamm et al., 1981) with relatively few as large as a million tons of ore or more, such as the Sunday and Deremo Mines. The average ore grade is 0.25 percent U_3O_8 and 1.25 to 1.50 percent V_2O_5 (Thamm et al., 1981).

Most of the emphasis of this study focused on the Sunday and the Deremo mines. The Sunday Mine is on the southwestern limb of the Gypsum Valley anticline six miles northwest of Gyp Gap (Figure 1). Sagging of bedding due to dissolution and collapse of the salt

domes produced small anticlines along the limbs as seen in beds along the southwestern limb that dip at 25 degrees both northeast and southwest. Faults cut the rim of the anticline along blocks that dropped into the collapse valley. The Sunday Mine deposit has been mined since the 1950's and includes five mines, the GMG, the Sunday, the Carnation, the St. Jude, and the West Sunday to the northwest. In total this mine complex has produced 942,000 tons of ore with an average of 0.19 % U_3O_8 and 1.36 % V_2O_5 (Hollingsworth, written communication, 1992). The Deremo Mine is 5.5 miles west of Egnar, Colorado on the Colorado-Utah border (Figure 1). In the vicinity of this mine, the Salt Wash Member is flat lying, and is cut by no major fault. Multiple levels of the Salt Wash Member were mined at the Deremo Mine which has operated since 1959. The Deremo deposit has produced 1,980,000 tons of ore with an average grade of 0.17 % U_3O_8 and 1.61 % V_2O_5 (Hollingsworth, written communication, 1992). Both the Sunday and Deremo ore deposits are below the water table hence the primary ore minerals have not been oxidized.

EXPERIMENTAL

FIELD STUDY

Five mines in the Uravan mineral belt were visited to examine the red-white sandstone boundaries. The mines were CSR-15, the Cougar, the La Sal, the Sunday, and the Deremo (Figure 1). The stopes and drifts surrounding the exposed red sandstone were mapped in each mine. The features mapped included the red-gray-green sandstone boundaries, cut and fill mudstone layers, ore geometries, and detrital carbonaceous trash. The La Sal and CSR-15 Mines were dropped from this study because of the absence of red-white sandstone boundaries and the abnormally high pyrite concentrations within the sandstone, respectively.

Because of the close proximity of red-gray-green sandstone exposures with ore, the Sunday, the Deremo Mines, and the Cougar Mine were selected for this study. The Sunday Mine was the focus of this study because a tongue of red sandstone was found in the center of the development drift leading to stope 1882 and has ore on both ends of the drift (Figure 4). Samples from the Sunday Mine were taken at 1 to 2 meter intervals, across the contact of red and gray-green sandstone from the east end of the development drift in stope 1882 (Figures 4 and 5). A sample of red sandstone from the west

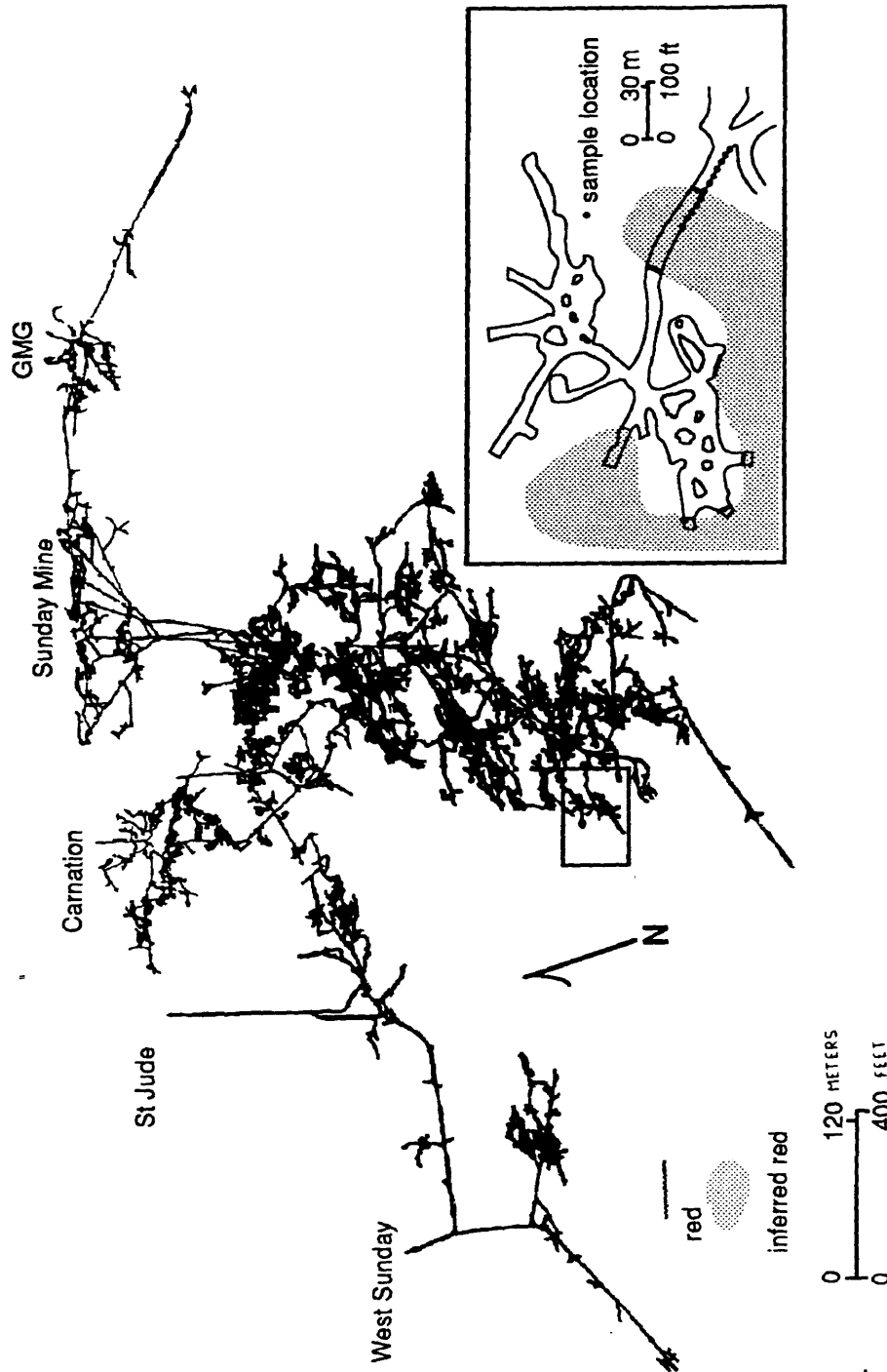


Figure 4: Plan view of the Sunday Mine workings and enlargement of stope 1882, showing distribution of known red sandstone.

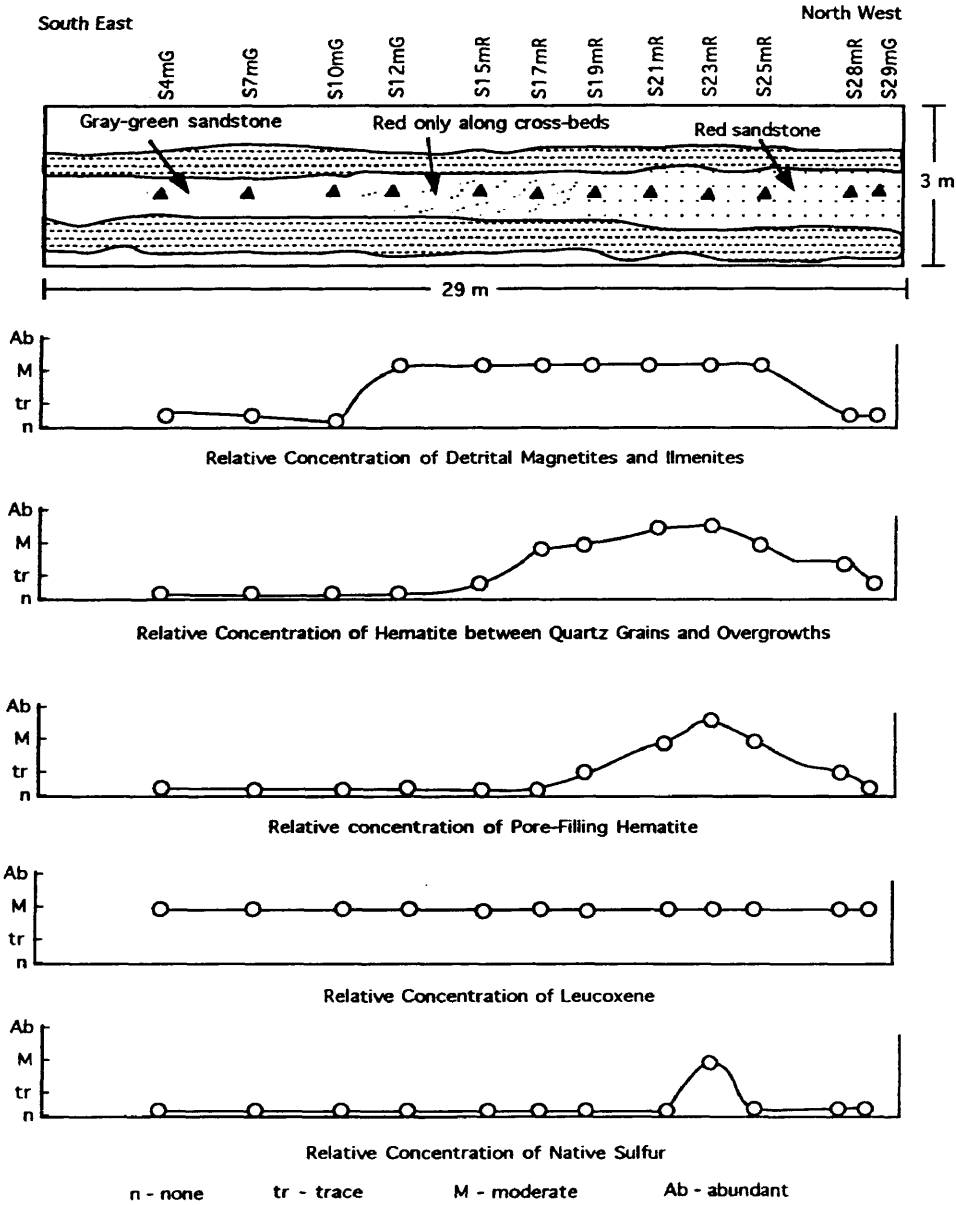


Figure 5: Map of the south rib of drift leading to stope 1882, Sunday Mine, and graphs showing the relative concentrations of key phases across the drift.

end of stope 1882 was collected to compare with red rocks found along the east end drift (Figure 4). The Deremo Mine was selected for study because the entire west side of the deposit is known to grade into red sandstone. Samples from the Deremo Mine were taken along a northwest trending rib of exposed red sandstone (Figures 6 and 7). The Cougar is a shallow mine and oxidation prevented detailed studies. However a few samples from the Cougar Mine were collected for comparison. Surficial red sandstone samples were collected from outcrop in Cougar Canyon on Horse Range Mesa. In addition, a sample of red Salt Wash Member sandstone, at least 600 meters from any known vanadium-uranium deposit, was collected from one of the Atomic Energy Commissions 1950's drill cores, DV-120 (Figure 1).

LABORATORY STUDY

The color, composition and petrographic characteristics of the rocks were described in the laboratory. Colors of the samples were determined using the standard colors of the Geological Society of America rock-color chart (Goddard et al., 1948), interpolating when necessary. Thin sections were prepared from samples impregnated with blue epoxy. Samples were examined in transmitted and obliquely reflected light (Adams et al., 1974) with a standard petrographic microscope, to identify transparent and opaque

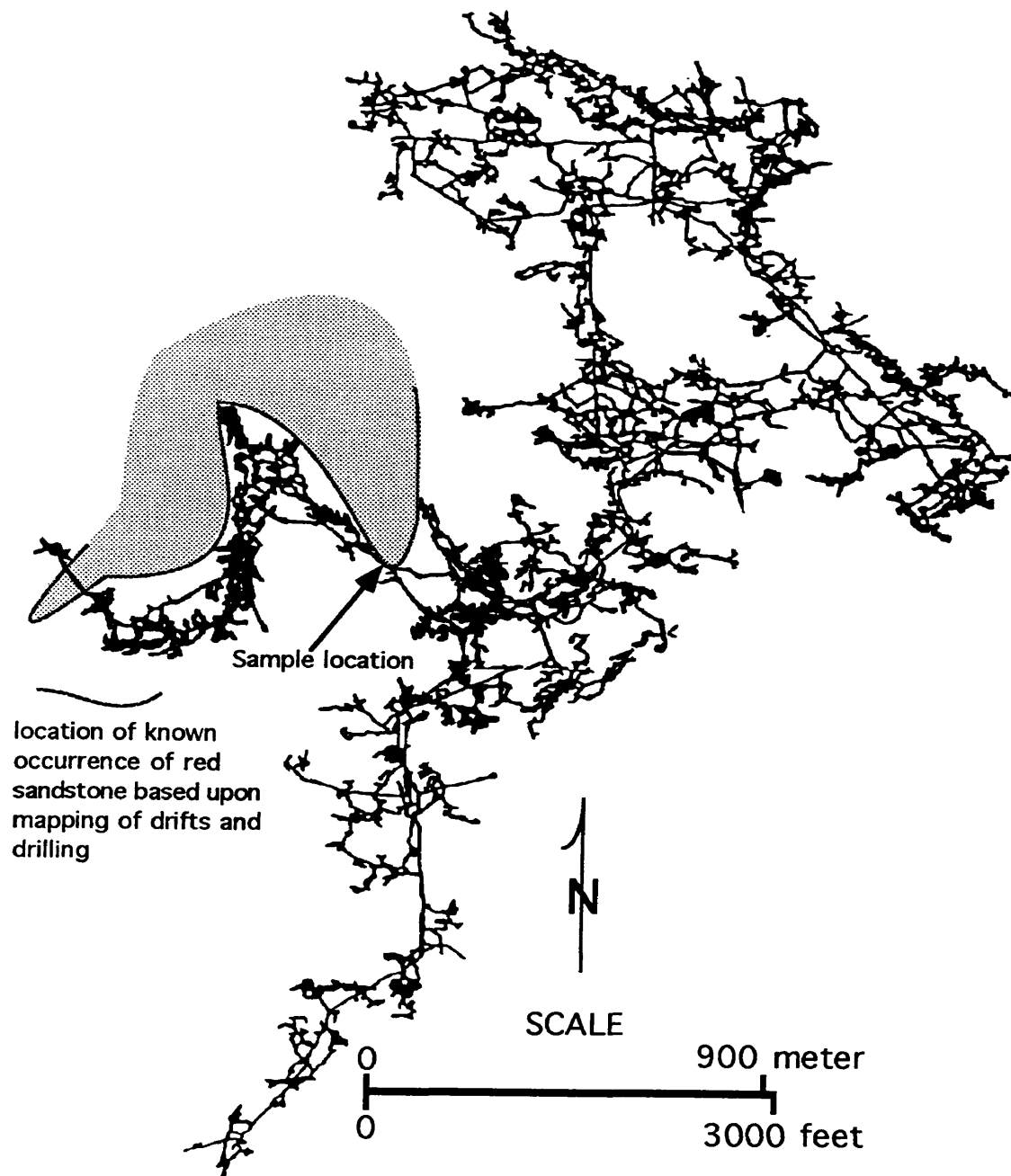


Figure 6: Plan view of the Deremo Mine, showing distribution of known red sandstone and sample locations (modified from Thamm et al., 1981).

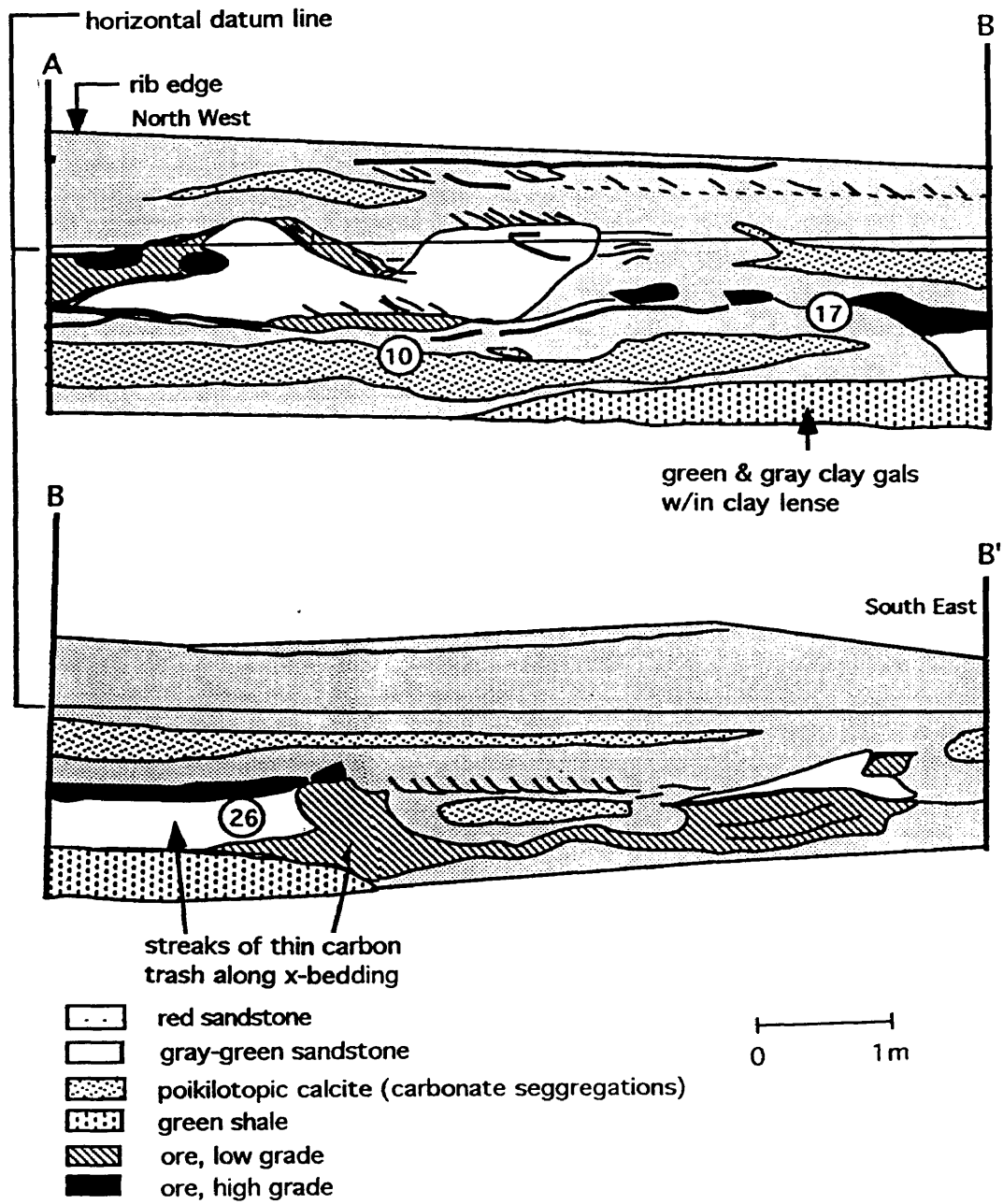


Figure 7: Map of the northeast rib showing sample locations, located in Figure 6, Deremo Mine.

minerals, and fabric. Based upon petrographic data a paragenetic sequence was determined. Polished thin sections were made of selected samples to identify the opaque minerals. Rock chips were carbon coated and examined with a scanning electron microscope (SEM) to refine paragenetic relations and examine very fine-grained phases. The SEM was a Cambridge Stereoscan 250 Mk2 equipped with a LaB₆ filament. To obtain qualitative compositions of the phases examined, a Tracer Northern Energy Dispersion Spectrometer unit was used (EDS). Petrographic and SEM data for all samples are tabulated in the Appendix.

RESULTS

Maps of the location and extent of red sandstone in the Sunday and Deremo Mines are presented in Figures 4 and 6. In the Sunday Mine, the walls of the drift leading to stope 1882 are composed of mainly red sandstone. Sandstone samples were collected between two mudstones that cross the length of the drift, one 0.5 m and the other 1.5 m above the floor. These mudstones are mottled green and red but are mainly green. The boundary between red and gray-green sandstone along the length of the drift is gradational, ranging from entirely gray-green, through a transition zone with minor red pigment (hematite) that is found only along some cross-beds, to a

sandstone that is homogeneously red (Figure 5). Sample S29mG was taken from the boundary between red sandstone and an isolated area of gray-green sandstone. The red samples from the Deremo and the Sunday Mines have an uneven distribution of red along cross beds, while the red samples from Horse Range Mesa and the core DV-120 are uniformly red sandstone. Organic matter was not identified in any of the samples but within a few meters of red sandstone in the gray-green sandstones of the Sunday and Deremo Mines and on Horse Range Mesa carbonized detrital plant fragments were found.

The color of samples from the Sunday Mine grade from a light greenish gray (5GY 9/1), sample S4mG, to increasing hues of red (5 to 10R), then back to down to light olive gray (5Y 6/1), in sample S29mG as the drift is crossed. The darkest red in samples S15mR to S28mR is found along argillaceous cross-beds. Rock color of samples from the Deremo Mine and drill core are similar to those of the Sunday samples (Appendix).

The fabric of the Sunday samples correlates with the presence of hematite. Gray-Green samples are well sorted, while the reddest samples, S19mR, S21mR, and S23mR, are only moderately sorted. Pore-filling clay was found in both red and gray-green sandstones, but is more common in red sandstone (S17mR, S19mR, S21mR, and S23mR). Based upon textures seen in the SEM, the pore-filling clay is partly authigenic and partly detrital but their relative abundance is unknown. Pore-filling clay in red sandstone has a core that is

commonly intermixed with very fine-grained hematite, and also an outer rim with no hematite (Figure 8). Most gray-green and some of the light red samples have epoxy inclusions within feldspars and quartz grains (Figure 9)

Hematite is responsible for the color of all red sandstones. Of the Sunday Mine samples, the highest concentrations of hematite, estimated visually, are found in samples S19mR, S21mR, S23mR, S25mR. Within these sandstones, hematite occurs as inclusions in authigenic minerals, coating on detrital grains such as along the boundaries of detrital quartz grains and quartz overgrowths, along fractures within quartz grains, between quartz grains and carbonate cements (Figure 10), and submicron grains that stain pore-filling clay (Figure 8), rock fragments, and leucoxenes (Figure 11). Original outlines of grains that have been replaced by quartz or calcite are commonly marked by hematite (Figure 12). The hematite that coats on some grains is so small that discrete grains are $<0.1 \mu\text{m}$ and could not be resolved by SEM. A few grains with large iron concentrations were detected with backscatter imaging. Individual hexagonal platelets of hematite (Figure 13) occur within clay, quartz and calcite. The gray-green samples have trace amounts of hematite only in zones of low permeability, such as under quartz overgrowths. The habits of hematite in the Sunday Mine samples are identical to those of the Deremo Mine, Horse Range Mesa, and core DV-120.

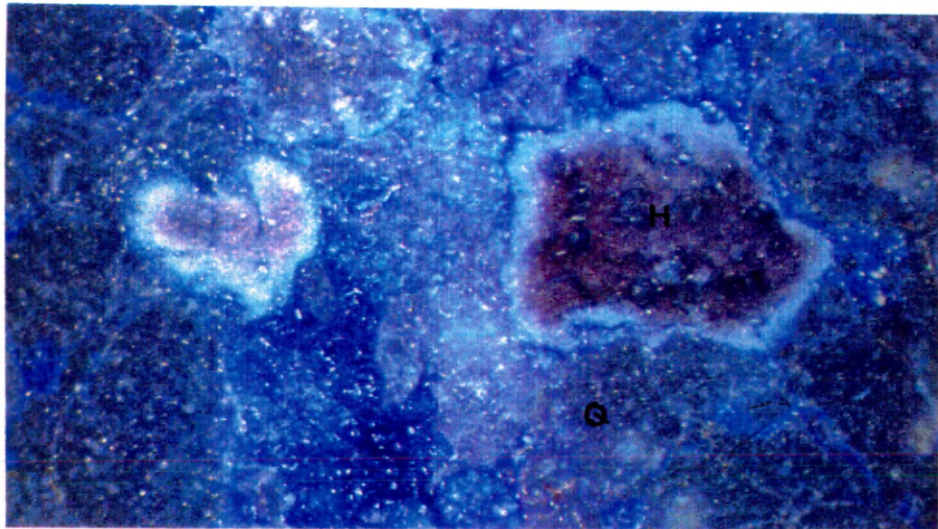


Figure 8: Photomicrograph in oblique reflected light of pore-filling clay coated with amorphous pigmentary hematite (H) and surrounded by detrital quartz grains (Q). Hematite has been removed from edges of pore-filling clay. Field of view = 1.0 mm wide.

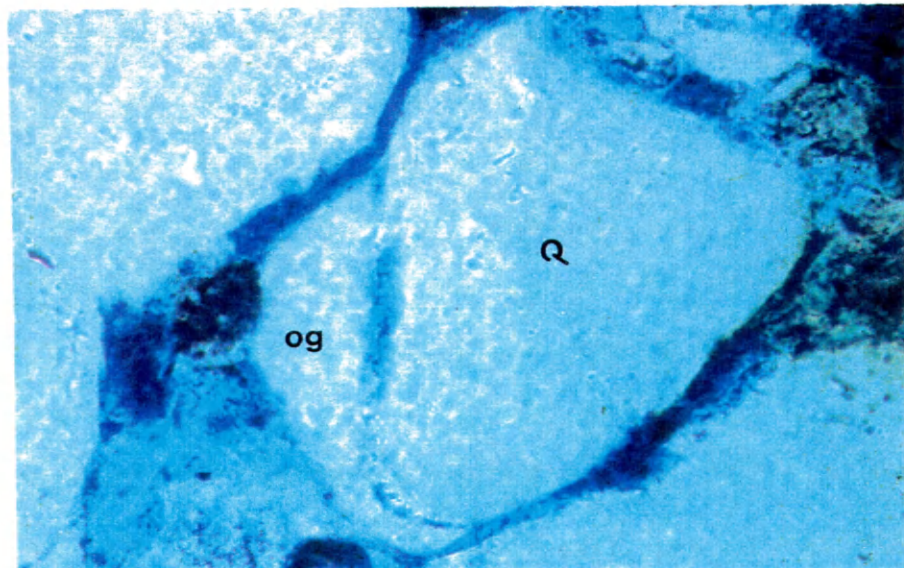


Figure 9: Photomicrograph in transmitted plane polarized light of void space filled with blue epoxy between detrital quartz grain (Q) and quartz overgrowth (og). Field of view = 0.2 mm wide.

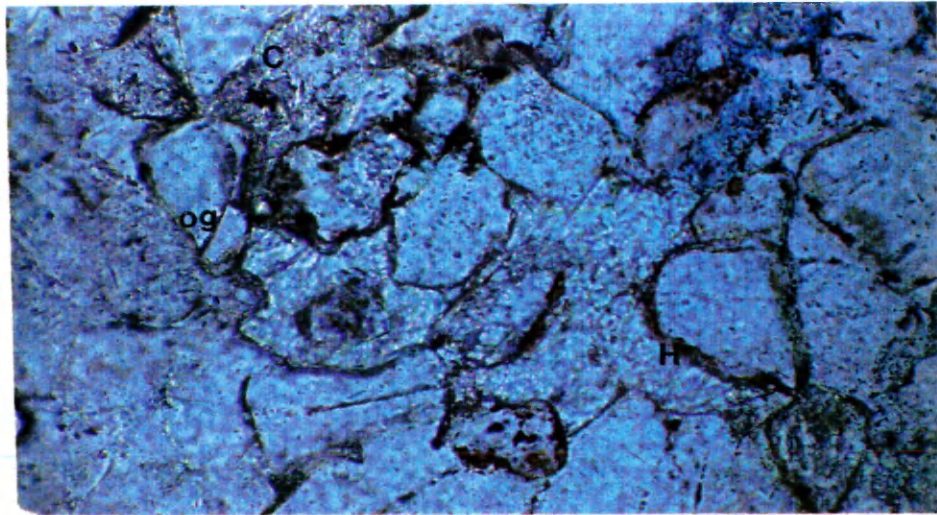


Figure 10: Photomicrograph in transmitted plane polarized light of hematite (H) within quartz overgrowths (og) and between overgrowths and calcite (C). Field of view = 0.5 mm wide..

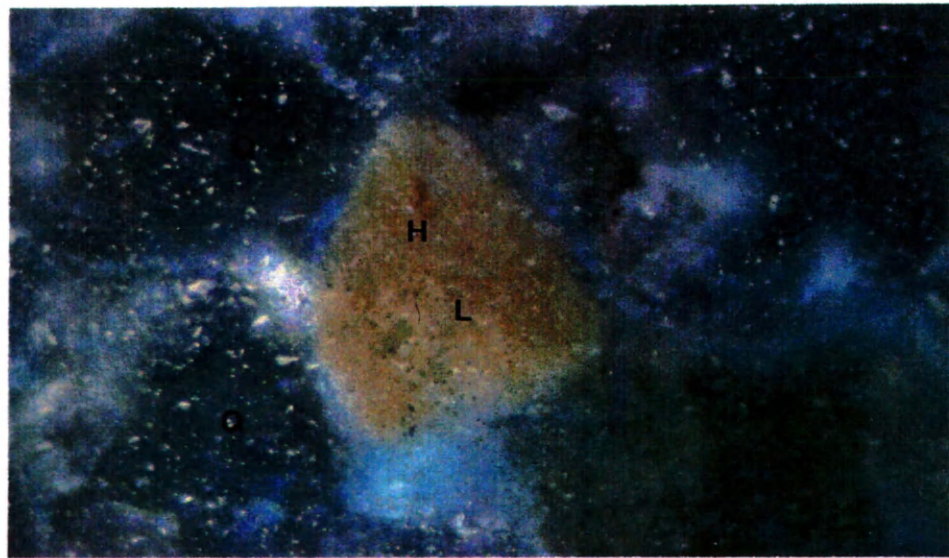


Figure11: Photomicrograph in oblique reflected light of hematite (H) coating authigenic leucoxene (L). (detrital quartz grain (Q)). Field of view = 0.2 mm wide.

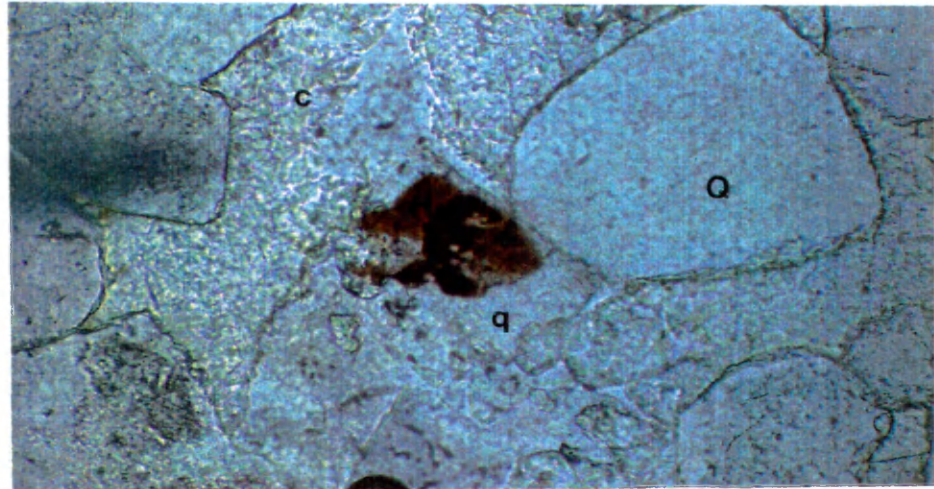


Figure 12: Photomicrograph in transmitted plain polarized light of detrital grain stained with hematite (H) subsequently replaced by quartz (q) and carbonate (c) cement. (detrital quartz grain (Q)). Field of view = 0.5 mm wide.



Figure 13: Photomicrograph in oblique reflected light of hematized detrital magnetite grain (Hm), hematite within quartz overgrowth (H) and detrital quartz grains (Q). Field of view = 0.2 mm wide.

Detrital magnetites and ilmenites, about 0.12 mm in diameter, were identified in thin section (Figures 14 and 15) and by SEM (Figure 16). SEM identification was based upon iron abundances and the round, pitted grain surfaces. These pitted grain surfaces are the results of etching that is typical of fluvial transport (Boggs, 1987). Red and gray-green sandstones from all locations contain some detrital magnetites and ilmenites but they are more abundant in red sandstones. Most grains are rounded and they are most abundant along cross-bedding laminae. The relative concentrations were visually estimated, and are consistent with estimates of Bowers and Shawe (1961) who determined that red sandstones contain about 0.2 percent black opaques and gray-green (altered) sandstones have 0.002 percent black opaques. Detrital magnetites and ilmenites in red sandstones are commonly partially replaced by hematite (Figure 14). Partially dissolved ilmenites commonly have hematite intergrown with leucoxene. This hematite is considered authigenic, because of the similarities between the textures of the hematite and the exsolution laminae of detrital magnetite and ilmenites. Some hematized magnetite grains are loosely packed, spongy (Figure 17) or have jagged edges, which distinguishes them from the rounded edges of the original detrital grains.

Pyrite occurs in both red and gray-green sandstone. A few red sandstone samples contain trace amounts of pyrite. This pyrite is

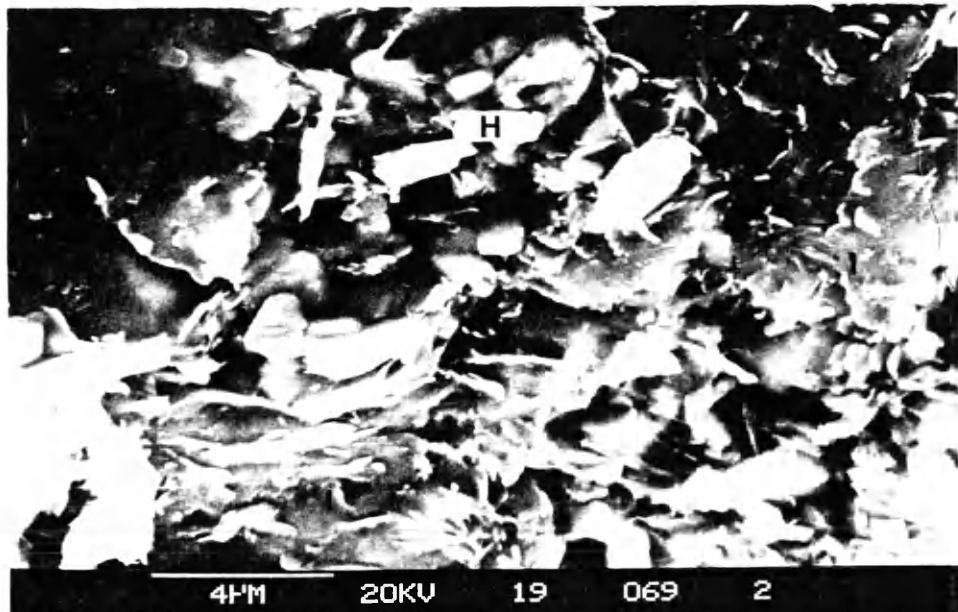


Figure 14: SEM micrograph of hematite crystals (H) within illite (I).

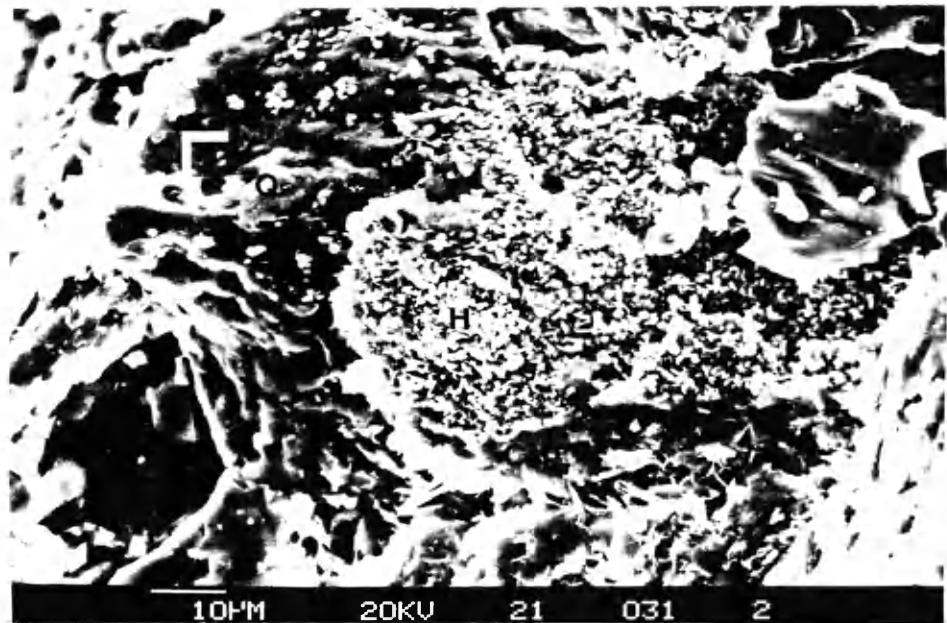


Figure 15: SEM micrograph of aggregates of hematite crystals (H) with quartz (Q) and authigenic chlorite (CHL)

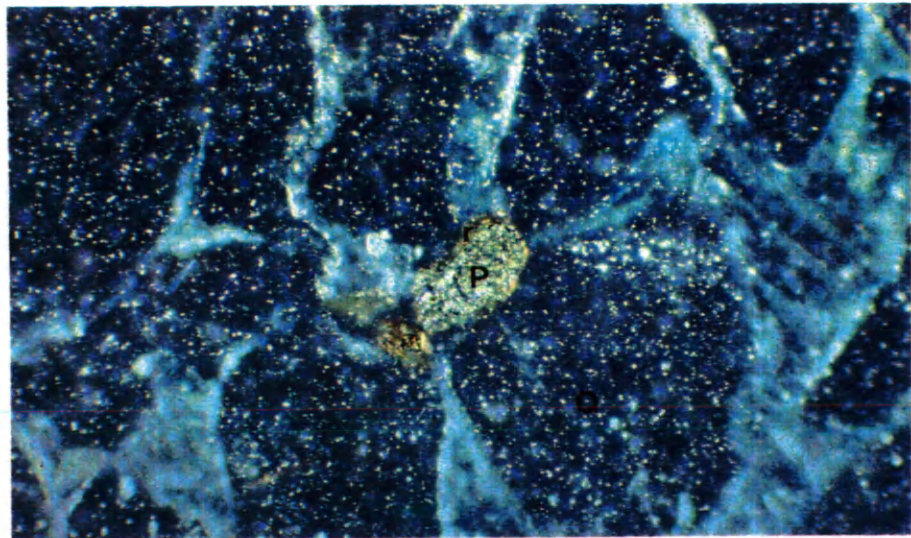


Figure 16: Photomicrograph in oblique reflected light of authigenic subhedral pyrite (P) with reaction rim (r), surrounded by detrital quartz grains (Q). Field of view = 0.5 mm wide..

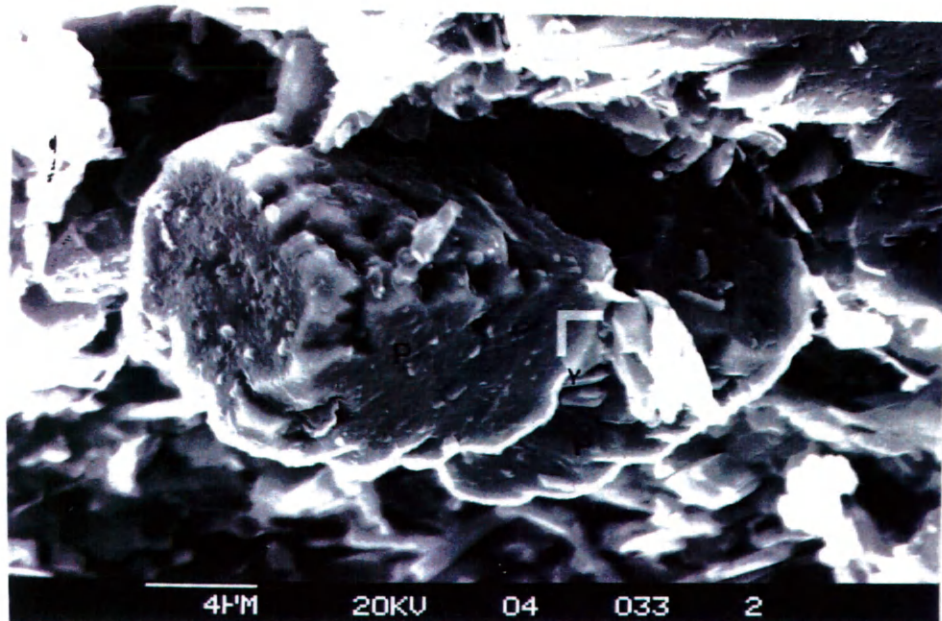


Figure 17: SEM micrograph of pyrite cubes (P) that are partially dissolved on top and bottom faces.

platy (Figure 18) and shows no evidence of corrosion. Euhedral to subhedral pyrite has been found in the following samples, S1R, S4mG, S19mR, and S29mG (Figures 18, 19 and 20). A reaction rim, of unknown composition, was found around a subhedral pyrite grain (Figure 19). Pyrite cubes in gray-green sandstones have been partially dissolved, as indicated by corroded top and bottom faces (Figure 20). Pyrite is also a component of samples from the Deremo Mine and Horse Range Mesa but not DV-120.

Authigenic TiO_2 phases identified in obliquely reflected light are all grouped together as leucoxenes, due to the lack of different optical properties between microcrystalline TiO_2 , anatase, and brookite (Adams et al., 1974). Spherical grains, up to 0.12 mm in diameter (Figures 11 and 21) and irregularly shaped fragments (Figure 22) of leucoxene are common. Irregularly shaped fragments are often cemented with calcite, or are inclusions within or on the surfaces of quartz overgrowths (Figure 22). Small inclusions of leucoxene are found in feldspar grains (Figure 23), rock fragments and chert. Leucoxenes are commonly intergrown with or rim magnetites and ilmenites (Figure 15). Figure 24 exhibits a porous aggregate of microcrystalline TiO_2 . Flakes and sheets of TiO_2 were also identified. Compositionally the porous microcrystalline and sheet-like TiO_2 grains are distinguished by the greater iron abundances of the microcrystalline variety. Porous microcrystalline TiO_2 is also trapped between quartz grains and quartz overgrowths

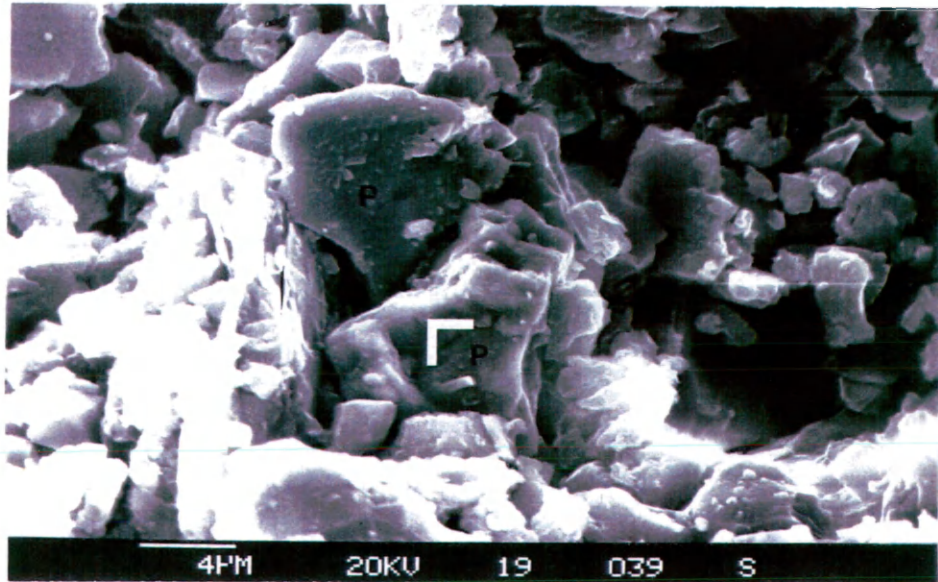


Figure 18: SEM micrograph of pyrite (P) with a platy morphology

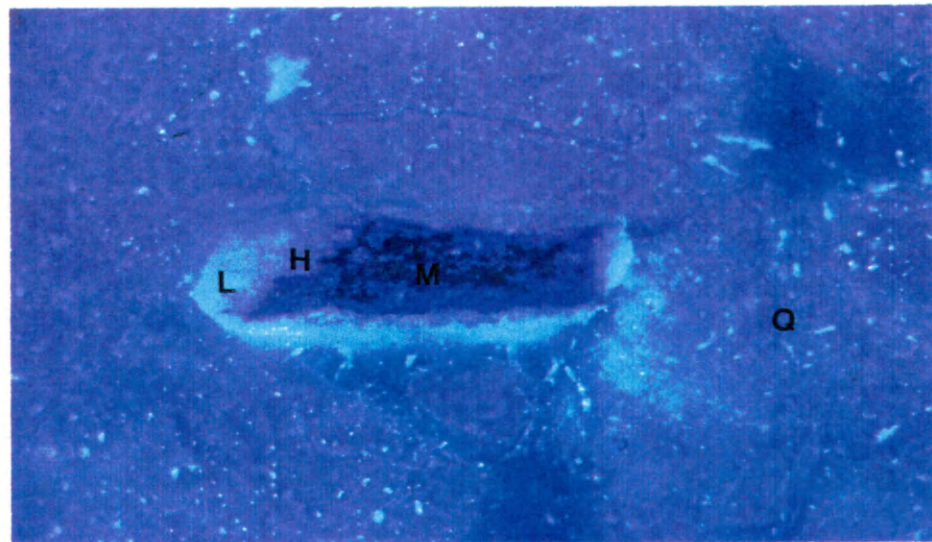


Figure19: Photomicrograph in oblique reflected light of detrital magnetite (M) partially altered to hematite (H) and leucoxene (L). Surrounded by detrital quartz grains (Q). Field of view = 0.2 mm wide.

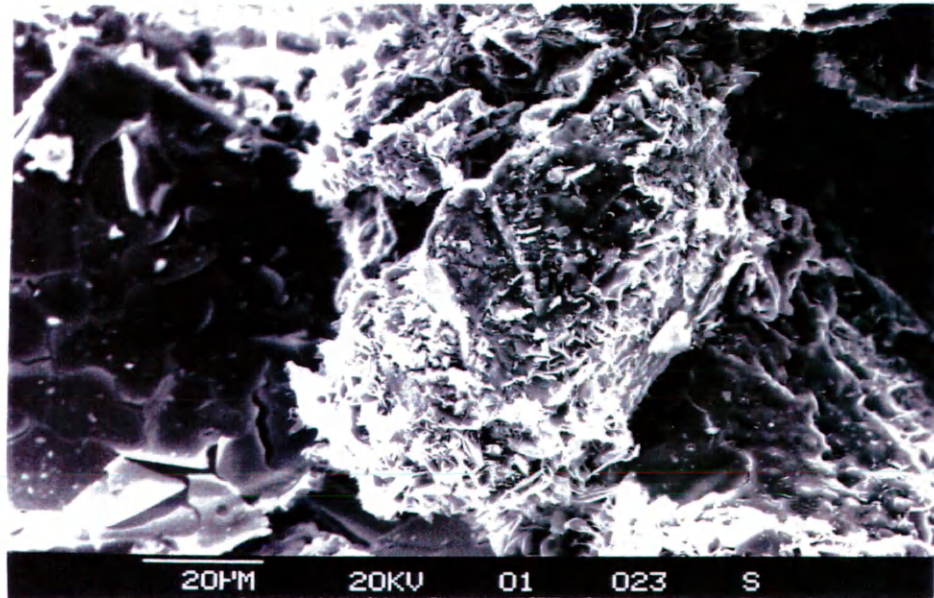


Figure 20: SEM micrograph of detrital titanomagnetite grain (tM).

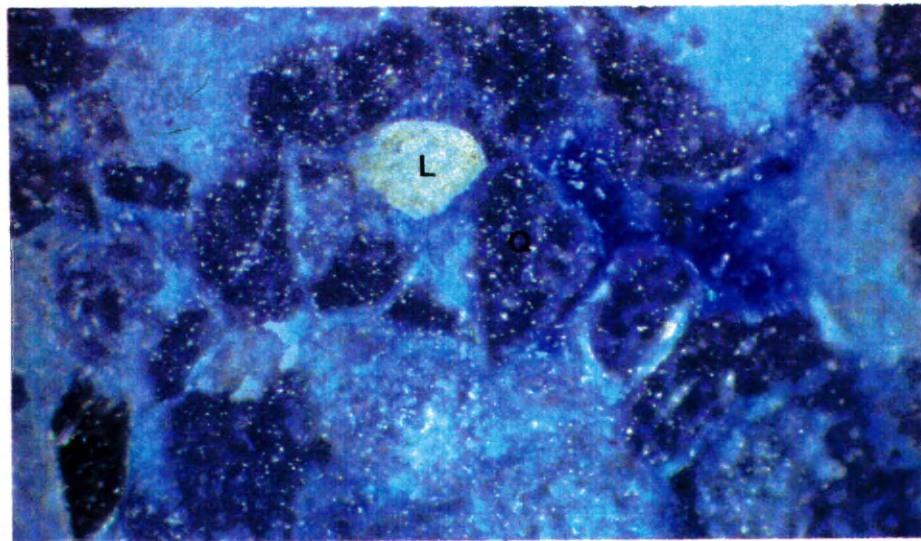


Figure 21: Photomicrograph in oblique reflected light of authigenic spherical leucoxene grain (L), partially altered angular detrital magnetite grain (M), and detrital quartz grains (Q). Field of view = 0.5 mm wide..

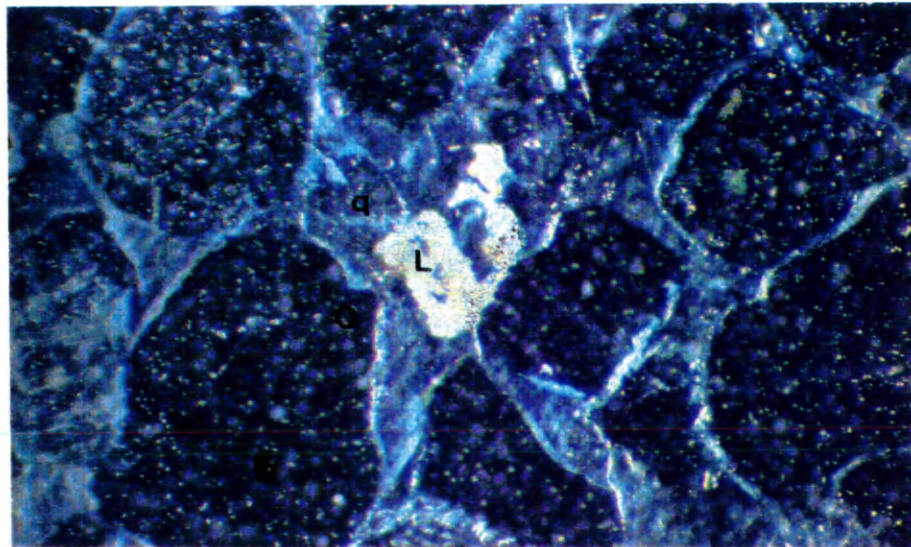


Figure 22: Photomicrograph in oblique reflected light of angular authigenic leucoxene grain (L), surrounded by quartz cement (q), and detrital quartz grains (Q). Field of view = 0.5 mm wide..

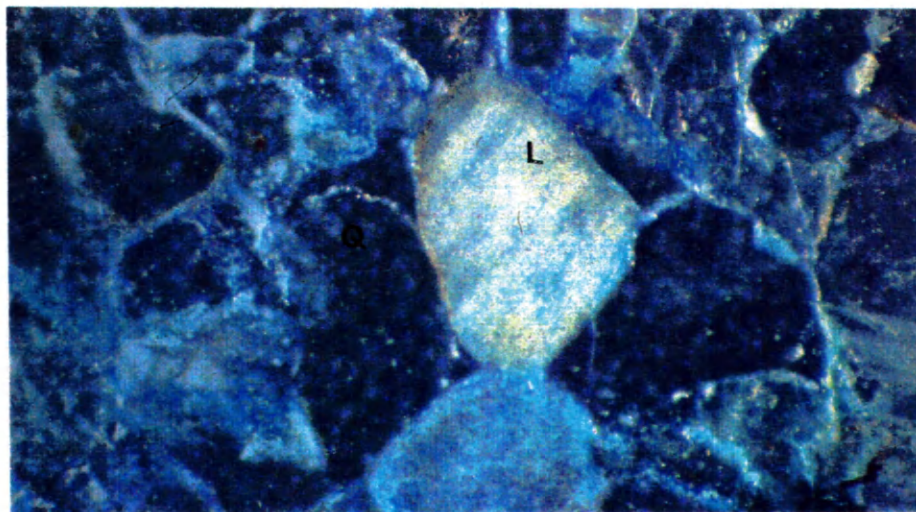


Figure 23: Photomicrograph in oblique reflected light of partially dissolved detrital feldspar grain with inclusions of leucoxene (L) and detrital quartz grains (Q). Field of view = 0.5 mm wide..

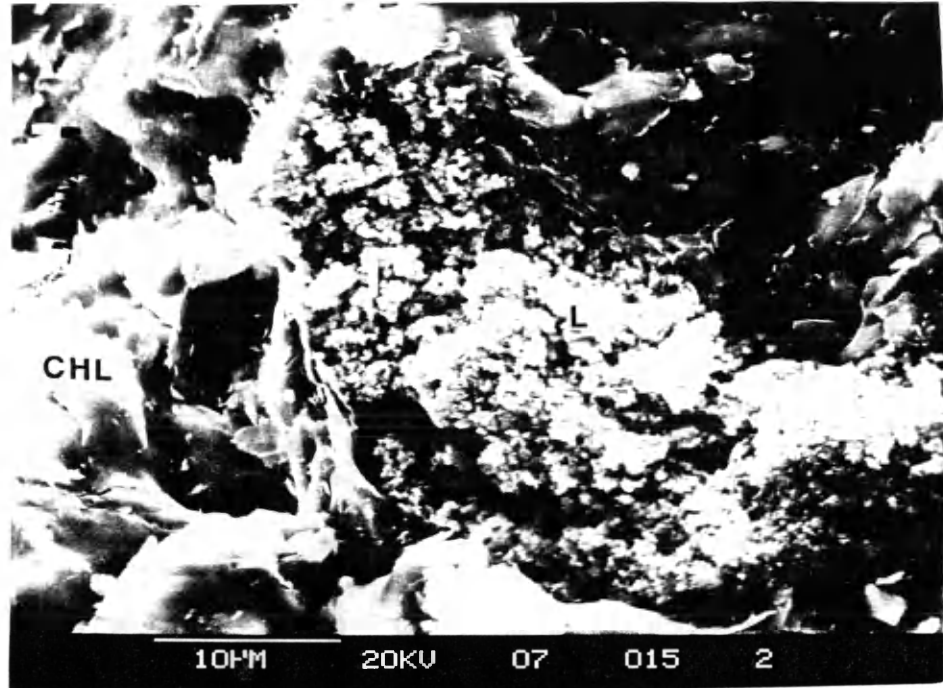


Figure 24: SEM micrograph of leucoxene grain aggregate (L) surrounded by chlorite (CHL).

(Figure 25). Prismatic and rhombohedral crystals resembling brookite (Morad and Aldahan, 1986), and orthorhombic and pyramidal anatase crystals are present in both red and gray-green sandstones. Leucoxene commonly contains crystals of hematite. The only difference between red and gray-green sandstone involving authigenic TiO_2 is that gray-green samples have TiO_2 commonly intergrown with chlorite and illitic material while in red sandstones TiO_2 is commonly stained with hematite.

Native sulfur was found in only the Sunday Mine and only in one red sample. Multiple occurrences of native sulfur in sample S23mR was confirmed by EDS. The sulfur crystals were bladed. These native sulfur grains are located along the cross-bedding laminae where the concentration of hematite is highest.

Authigenic cements, such as quartz, chert and chalcedony, calcite and gypsum, are common throughout the Salt Wash Member. The most abundant authigenic cement in all samples is quartz as overgrowths. Quartz overgrowths occur in red and green sandstone but are more easily recognized in red sandstone, due to the presence of red bubbles and hematite inclusions along the contacts between detrital grains and the overgrowths. Chert and chalcedony are found in red and gray-green sandstone as grains and pore-filling cement. Calcite and barite are evenly distributed in both red and gray-green sandstone as pore-filling cement and poikilotopic segregations. Unlike the other authigenic cements, gypsum was found only in the

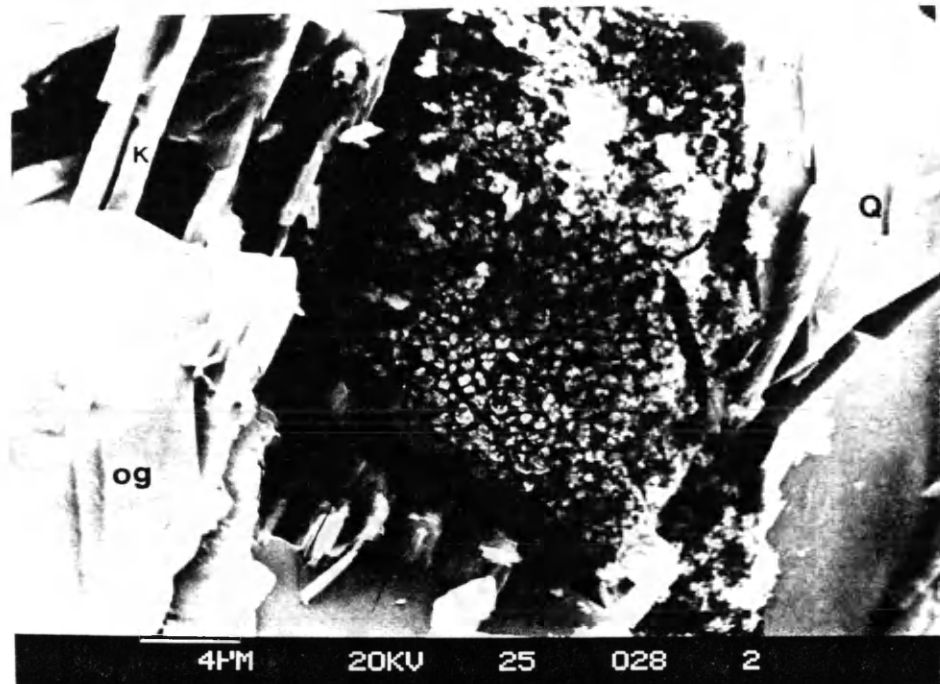


Figure 25: SEM micrograph of microcrystalline leucosene between detrital quartz grain (Q) and quartz overgrowth (og), and partially dissolved K-feldspar (K).

Sunday Mine in the red sandstone samples S17mR, S19mR, and S21mR as a poikilotopic and pore-filling cement.

DISCUSSION

The formation of red and gray-green sandstones near vanadium-uranium deposits, are the result of three stages of alteration characterized by two different pore-water compositions. Some of the sandstones near the red gray-green sandstone boundary were subjected to reducing conditions, oxidizing conditions, and were then re-reduced. This three stage scenario was based upon the field and petrographic relationships of the authigenic and altered mineral assemblages identified in both red and gray-green sandstone. A paragenetic sequence (Table 2) explains the formation of the authigenic and altered phases in three diagenetic stages, shallow burial I, shallow burial II, and deep burial. In the discussion, the terms oxidation and reduction refer to the oxidation state of iron in the authigenic minerals.

Table 2: Paragenetic sequence of authigenic phases in the Salt Wash Member of the Morrison Formation associated with oxidation in the Slick Rock district.

Minerals	Shallow Burial Early	Shallow Burial Late	Deep Burial
Quartz	precipitation of pore-filling chert, chalcedony	continue	continue & quartz precipitation
Calcite	none	none	precipitation as pore-filling & poikilotopic cement, around hematite
Pyrite	precipitation	dissolution in permeable sands by oxygenated water	precipitation
Leucoxenes	forms from leaching Fe(II) from magnetite & ilmenites	continues slower in oxygenated fluids	continues for short time
Iron Oxides	none	precipitation on quartz grains, stains leucoxene, alters magnetites & ilmenites	recrystallization to hematite, no further precipitation but partial dissolution
Native Sulfur	none	none	precipitation during reduction of iron oxides
V-U Minerals	none	vanadium-uranium carried in oxic fluids and accumulated by reductant	recrystallization?

Shallow Burial

The Salt Wash Member was deposited under seasonally wet and dry conditions, a monsoonal climate (Tyler and Ethridge, 1983). The seasonal aeration of the sediment, due to fluctuations in the water table, caused a corresponding change in the reduction potential of the pore-waters. The amount of water table drop, and subsequent aeration, was variable across the depositional surface and controlled by paleogeography and drainage patterns. The drainage patterns differ significantly between the overbank mudstone and the channel sandstone. The relatively elevated Salt Wash Member overbank mudstones were deposited under iron oxidizing conditions (Shawe et al., 1968; Breit, 1986). Although large portions of the Salt Wash Member were oxic, some channel sandstones like those that contain ore were reducing. The preservation of plant fragments in the channel sandstones of the Sunday and Deremo Mines, indicate that portions of channel sandstones did remain iron-reducing, even during the seasonal times of a low water table. The continuous reducing conditions within the sandstones are attributed to the drainage of oxygen-depleted floodplain sediment pore-waters into the channels, dissolved organic matter near buried plant fragments, and bacterial activity. No organic matter was identified in the samples examined, but carbonized logs and smaller plant fragments are found throughout the mines.

Shallow Burial I

The shallow burial I stage defines the iron reducing conditions that were present near detrital organic matter. This included the entire section in the Deremo and Sunday mines. The iron reducing pore-waters were oxygen poor, rich in organic matter and probably slightly acidic. Bacteria were active in these sediments. These reducing pore-waters dissolved iron from magnetite and ilmenite and formed pyrite. Detrital magnetites and ilmenites were completely altered only in sandstones that remained reducing during the oxidation, shallow burial II stage. The shallow burial I episode is comparable to Shawe's (1976) carbon facies.

One of the greatest compositional differences between the gray-green and red sandstones is the removal of iron from some ilmenites and magnetites leaving residual leucoxenes. Previous experimental studies have defined general conditions favorable for dissolution of iron and iron-titanium oxides. Lynd (1959) found that the most effective agents of ilmenite dissolution were humic acid and sulfuric acid, while weakly alkaline solutions had no apparent effect. Gruner (1959) found that ilmenites alter to TiO_2 , FeS and FeS_2 when subjected to heat and hydrogen sulfide. Carroll (1959) and Austin (1960) found that ilmenites in reduced sediments altered to authigenic rutile, anatase, pyrite and siderite. Miller and

Folk (1955), while studying reduction zones in red beds, found that the concentration of magnetite and ilmenite is lower in reduced sandstone, as compared to magnetite and ilmenites in the red oxidized sandstone. Miller and Folk (1955) felt that reducing solutions dissolved the magnetites and ilmenites. Thus dissolution of magnetites and ilmenites in channel sandstones near organic matter records early reducing solutions.

The other mineral, typical of the shallow burial I stage, is pyrite. Pyrite is found in almost all gray-green samples in trace amounts. Precipitation of pyrite at low temperatures in a shallow burial setting is typically bacterially controlled (Goldhaber and Kaplan, 1974; Postgate et al, 1982). A bacterial origin is confirmed by the light isotopic composition of sulfur in the sulfide minerals of the vanadium-uranium deposits (Breit, 1986; Jensen, 1958). The sulfate-reducing bacteria require organic matter, which in the Salt Wash Member sandstones included dissolved organic matter from the degradation of plant fragments deposited with the sediments. The presence of pyrite documents the presence of H₂S and dissolved organic matter as components of the reducing solutions.

The low concentration of magnetite and ilmenite in the gray-green sandstone may have been partially a result of the lower pH in gray-green sandstone than in red sandstones. A low pH in these sandstones is consistent with bacterial activity, specifically sulfate reduction, which can lower the pH of alkaline waters to

between 6 and 7 (Gardner, 1973; Birnbaum and Wireman, 1984). The lower pH is due to the generation of CO₂ from the degradation of organic matter during sulfate reduction.

Shallow Burial II

The shallow burial II stage defines the introduction of oxic water into the reduced channel sandstones. The alteration and partial dissolution of pyrite in now red and gray-green sandstones is consistent with the iron-reducing conditions existing prior to iron-oxidizing. This water passed through the Brushy Basin Member and carried dissolved oxygen, vanadium, and uranium. This fluid reddened the channel sandstone by oxidizing iron contained in unstable framework grains and reducing pore-waters. The incursion of oxidizing fluids began soon after the reducing conditions were established near the carbonaceous trash. During the shallow burial II stage, detrital magnetites and ilmenites were preserved and some oxidized while authigenic pyrites were dissolved. Also the dissolved vanadium and uranium in this solution were reduced and precipitated by reaction with reductant in the channel sandstone pore-waters. The sandstone reddened during the shallow burial II episode is comparable to Shawe's (1976) red-bed facies, although most of Shawe's red beds were never reducing. The oxidation

described here was focused in sandstones in which pore-waters typical of shallow burial I alterations were preserved. The iron oxidizing pore-water, that formed ferric oxides in the sandstone, is interpreted to have been introduced during shallow burial, because depositional waters of the Morrison are the only probable source for an oxygenated meteoric water.

The iron oxides formed during reddening are a product of oxidation of iron contained in minerals and reducing pore-waters altered by the oxic water. This is supported by the low mobility of Fe(III) in the range of most natural pH's (Stumm and Morgan, 1970). A likely iron source is Fe(II) dissolved from the alteration of magnetites and ilmenites by the local reducing conditions. The concentration of clay is higher in red than in gray green sandstones, and is also a possible iron source. Walker (1976) examined desert red beds in the southwestern United States and found that clays transported in suspension by percolating meteoric water supply adsorbed iron that is oxidized to hematite. Altered rock fragments in the Salt Wash Member are also an iron source; they commonly contain leucoxene, magnetite, ilmenite, hematite, and may have had Fe-rich silicates. The alteration of rock fragments has been so complete that the original rock type is obscured. Pyrite may have oxidized to form hematite, but was probably minor because pyrite is found only in trace amounts even in reduced rocks. Oxidized iron produced from these sources most likely precipitated as an iron

oxyhydroxide, such as ferrihydrite or goethite, and later altered to hematite (Pye, 1983).

Even though the red sandstone near the vanadium-uranium deposits sampled for this study was originally reducing with respect to iron, it contains high concentrations of magnetite and ilmenite. This requires incursion of oxic waters shortly after deposition otherwise the proposed reducing conditions of stage I would have completely leached iron from magnetite and ilmenite. Unaltered magnetites and ilmenites in the red sandstones are present but some are partially and totally hematized. These hematized magnetite and ilmenite grains commonly maintain textures resembling the exsolution laminae of the original grain indicating alteration of the detrital grain. Flinter (1959) and Lynd (1961) found that ilmenites altered to hematite by diffusion of oxygen during weathering but this alteration was hindered by alkaline solutions. Therefore, the only partial alteration of magnetites and ilmenites to leucoxene and hematite in red sandstone is attributed to the alkaline composition of the oxic waters. Additional evidence for an alkaline meteoric water is the authigenic mineral assemblage that is stable at a pH of 8 found in some iron deposits in the Slick Rock district (Breit and Goldhaber, 1989). Gallagher et al (1968) found that the oxidation of magnetite to hematite is a diffusion controlled reaction. If the oxidizing event persisted for a geologically short time, some of the magnetites

would remain unaltered. The limited supply of dissolved free oxygen necessary to oxidize the magnetite to martite could have limited hematization. Granger and Warren (1979) believe that the few ppm of dissolved free oxygen in meteoric water was consumed in oxidation reactions with pyrite, organic matter and ferrous iron minerals. This depletion of oxygen would limit the oxidation of magnetites and ilmenites to hematite and preserve reducing environments in which the vanadium-uranium ore formed.

The precipitation of vanadium and uranium in the deposits, as argued by Breit and Goldhaber (1989), occurred during shallow burial because of local low Eh pore-waters in certain channel sandstones. The oxidizing solutions that reddened the sandstones is also favored to supply vanadium and uranium in the deposits (Breit and Goldhaber, 1989). The incursion of oxidizing solutions into an area of reducing pyritic sandstones caused vanadium and uranium to precipitate. The depletion of dissolved oxygen in the water as it moved along the flow path did not affect transport of these metals until reducing conditions were encountered

The timing of sandstone reddening is constrained by the time of ore formation. Based upon recorded dissolved uranium concentrations within natural waters, sandstone hydrologic conductivity, and the size, tonnage and grade of ore from the Deremo Mine (Table 3), the time needed to generate a deposit the size of the Deremo Mine ranges from 2,000 years to 2.4 million years. Since the

Table 3: Parameters for the calculation of time needed for the generation of the Deremo Mine.

Deremo Mine *

Tons of ore: 1,980,000
Grade of ore: 0.17 % U_3O_8
Width of Mine: 2,161 m
Thickness of ore sand: 9.1 m

Concentration of dissolved U in natural waters**:
260 ppb to 0.02 ppb

Sandstone Properties***:

Hydrologic conductivity K: 10^{-1} to 10^{-2} cm/sec
Effective porosity: 10 %

Time range needed to generate the Deremo Mine:
2,000 years to 2.4 million years

*Hollingsworth, written communication, 1992

**Breit, personal commun., 1992

**Langmuir, (1978)

***Lerman, (1988)

Brushy Basin Member took 8 million years to be deposited (Imlay, 1980), there is plenty of time for the ore deposit to form and the reddening as well during the Brushy Basin Member deposition. The younger radiometric ages of 70 to 120 million years (Miller and Kulp, 1963; Breit, 1986) are likely a result of recrystallization of ore minerals (Breit,1986).

Ore in the Uravan mineral belt varies from tabular and peneconcordant with bedding to rolly (Thamm et al., 1981). Multiple horizons of ore are also found. These ore morphologic features could be formed by changing the shape or elevation of the reducing water table or the hydrologic gradient of the oxic meteoric water through time.

Besides the morphology, the major difference between the uranium deposits of Wyoming and Texas and the Uravan mineral belt, is the concept of rolls or the redistribution of ore once it accumulated. Evidence, like the absence or low concentration of detrital magnetites and ilmenites in red sandstone near ore compared to red sandstone away from ore (Saucier 1980) would suggest ore redistribution. No similar indications have been found in this study. In the Salt Wash Member, it is likely that the flux of oxygenated pore water varied with changes of precipitation. But even if the vanadium and uranium were slightly remobilized and redistributed due to hydrologic changes, it is doubtful that these minor changes would leave recognizable features, particularly

because the metals are believed to have recrystallized to their present, relatively immobile mineralogy during deep burial (Breit 1986).

Deep Burial

Recharge of the Salt Wash Member with oxidizing fluids had to stop with the increased depth of burial and deposition of overlying rocks with low Eh pore-waters. When the flux of oxygenated meteoric water into reduced sandstone ceased, reduced pore-water encroached into the reddened sandstone. Mudstone is the dominant lithology of the Brushy Basin Member and is up to 210 m thick. This lithology is impermeable and supports decreased recharge as the Brushy Basin Member was deposited. Even though the incursion of oxidizing pore-waters stopped, the iron reducing pore-waters were still being bacterially generated. Once the flux of oxidizing water ceased, these iron reducing pore-waters diffused into the reddened sandstone and dissolved hematite. The bleaching of red sandstone during the deep burial episode is comparable to Shawe's (1976) fault-related altered facies. The only difference is Shawe (1976) attributes the bleaching to reducing solutions traveling along faults while this study attributes bleaching to the local bacterial activity.

Evidence for re-reduction is apparent in the distribution of hematite. Hematite is found throughout some of the reddest sandstones under quartz overgrowth, lining pore space, replacing magnetites, and staining carbonates, clays, and leucoxenes. In the light color red sandstones altered by re-reduction, hematite is found only in areas of low permeability, such as under quartz overgrowths, clay-rich sandstones, and along cross bedding laminae. In the light red sandstones hematite does not line the vacant pore space like in the dark red sandstones. Also the pore-filling clay of the light red sandstones are stained with hematite, but have an outer rim of clay void of hematite. Sandstones with hematite preserved only along cross-beds contained hematite much like the darker red sandstones, therefore distribution of hematite is an indication that the rock has undergone iron-reducing conditions that dissolved the accessible hematite. The similarity between the location and shape of voids with and without hematite suggests that hematite has been leached from beneath some quartz overgrowths (Figure 8).

Partial dissolution of hematized magnetites was also a result of advancement of reducing pore-waters. As a result these grains are porous, loosely bound aggregates of hematite (Figures 13 and 15) (Bowers and Shawe, 1961; Shawe, 1976). Hematization must have occurred after deposition during the shallow burial II stage, because if the grains were hematized during transport, the initial reducing condition, identified in the shallow burial I stage would have

dissolved them. These grains were partially dissolved after compaction, because the porous grain aggregates are friable and would probably have been crushed during consolidation. The hematite grains were not totally dissolved because the deep burial re-reduction did not persist for a long enough period of time.

Leucoxene commonly contains inclusions of hematite or is stained by pigmentary hematite. The re-encroachment of reducing solutions into red sandstone, leached hematite from the porous, hematite-stained leucoxene grains. Other possibilities to account for the absence of hematite within leucoxenes in red rocks is that all the iron was dissolved during the shallow burial I stage, or that the leucoxene grains formed after the shallow burial II stage. The alteration of magnetites and ilmenites to leucoxenes is not considered a brief event, but occurred continuously from the time of transportation, to deposition, and deep burial.

In one of the reddest samples, native sulfur was found along cross bedding laminae with hematite. It is well documented that the reaction between hydrogen sulfide and a ferric oxide, such as goethite, produces pyrite with monosulfides, ferrous iron and native sulfur as intermediate products (Berner, 1970; Richard, 1974; Goldhaber and Kaplan, 1974; Stanton and Goldhaber, 1991). Thus native sulfur may be a product of reintroduction of H₂S bearing pore-waters into the reddened oxidized sandstones.

In addition to other evidence for the reintroduction of reducing fluids into the oxidized sandstones, it is speculated that disseminated porous microcrystalline TiO_2 grains are a product of the reduction and dissolution of iron oxides in the red sandstones. While experimenting with the extraction of iron oxides and iron oxyhydroxides from soils and sediments, Ryan and Gschwend (1991) discovered that the most efficient leaching method is a solution of dissolved Ti(III) complexed with citrate and EDTA buffered with bicarbonate. The reduction and subsequent dissolution of iron is accomplished by the oxidation of titanium(III) to (IV) valence, which is then hydrolyzed to TiO_2 . No crystalline TiO_2 was identified by x-ray diffraction of the residue, but is believed to have remained in solution as a colloid (Ryan and Gschwend, 1991; Hudson and Morel, 1989).

Iron oxides and oxyhydroxides could likewise have been dissolved and replaced by titanium(III) complexed with organic acids from the surrounding reduced Salt Wash Member sandstones. The microcrystalline TiO_2 layer under quartz overgrowths (Figure 25) and the TiO_2 aggregate grains found in pore spaces (Figure 24) appears to have a desiccation texture similar to mud cracks in a dry lake bed and are interpreted as redistributed TiO_2 . The titanium could be derived from dissolution of detrital magnetites and ilmenites by H_2S and organic acids. Titanium was soluble and mobile in the reduced sandstones as seen by the precipitation of

crystalline TiO_2 minerals such as brookite and anatase. Titanium oxides could then be preserved in confined pore spaces, such as under quartz overgrowths and clay-lined pores, as some type of titanium oxide or oxyhydroxide which then dehydrated. The precipitation of an iron oxyhydroxide, such as goethite, which then dehydrates to hematite (Pye, 1983) could be an analogous reaction to the formation of microcrystalline titanium oxides in some areas of the sandstones. The dehydration of a titanium oxyhydroxide to a titanium oxide during drying after sampling of the sandstone would produce the desiccation texture found in Figure 25.

Most of the authigenic cements, such as quartz, calcite, and barite, are uniformly distributed throughout red and gray-green sandstone and are interpreted to be after oxidation and re-reduction. The uniform distribution of these cements and their precipitation did not depend upon redox potential. For example, quartz, and carbonate typically contain grains and inclusions of hematite and leucoxene. Barite cementation of hematite and leucoxene grains was not identified in this study but has been identified by other workers (Shawe, 1976; Breit, 1986). Barite precipitation has been related to epigenetic fault controlled solutions (Breit et al., 1990)

IMPLICATIONS TO VANADIUM-URANIUM EXPLORATION

In the exploration for vanadium-uranium ore, whether or not ore will be found along red-gray-green sandstone boundaries depends upon the permeability of the sandstones after oxidation has ceased, and the duration of the re-reduction of the oxidized sandstones. If the permeability is low and re-reduction did not completely reduce the oxidized sandstone, red sandstones may be found a few meters from ore. On the other hand, if permeability is high and re-reduction completely reduced the oxidized sandstones, red sandstone may be found more distant from ore. An additional factor that regulates whether ore is found along or near red sandstone is whether or not the oxygenated meteoric fluid passed through and leached uranium from a volcanic ash-rich bed. Distinguishing between a red sandstone that was oxidized by a pore-water carrying dissolved vanadium and uranium versus a fluid that carried no vanadium or uranium is not possible from the data collected in this study.

CONCLUSION

The Salt Wash Member of the Morrison Formation along red-gray-green sandstone boundaries near vanadium-uranium deposits has experienced a series of changes in redox potential since burial. The sequence of diagenetic events relating to the oxidation of the Salt Wash Member are diagrammed in Figures 26 a, b, and c.

The channel sandstones of the Salt Wash Member were deposited under monsoonal conditions. The periodic lowering of the water table during dry episodes and aeration resulted in an oxidation of iron dissolved from altered minerals. Portions of these channel sandstones, however, remained reducing relative to iron even during the dry seasons. The iron-reducing conditions were the result of water saturation with dissolved organic matter and bacterially produced hydrogen sulfide as seen by the presence of detrital plant fragments and pyrite (Figure 26a). Detrital black opaque minerals, such as magnetite and ilmenite, were almost totally dissolved in sandstones in which these iron reducing conditions were sustained from soon after deposition through deep burial.

Oxygenated meteoric water percolated through the Brushy Basin Member and leached uranium. The dissolved uranium precipitated upon mixing with the reducing fluids (Figure 26b). The

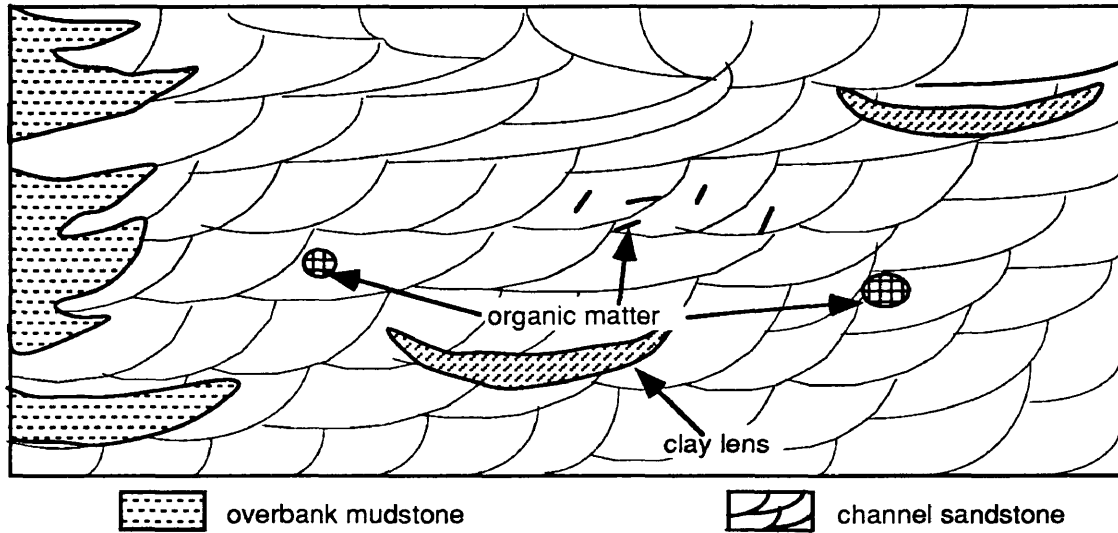


Figure 26a: Diagram summarizing the Shallow Burial I Stage with a portion of the channel sandstone remaining reduced due to dissolved organic material and bacterial activity. Channel sandstone is approximately 100 m wide. .

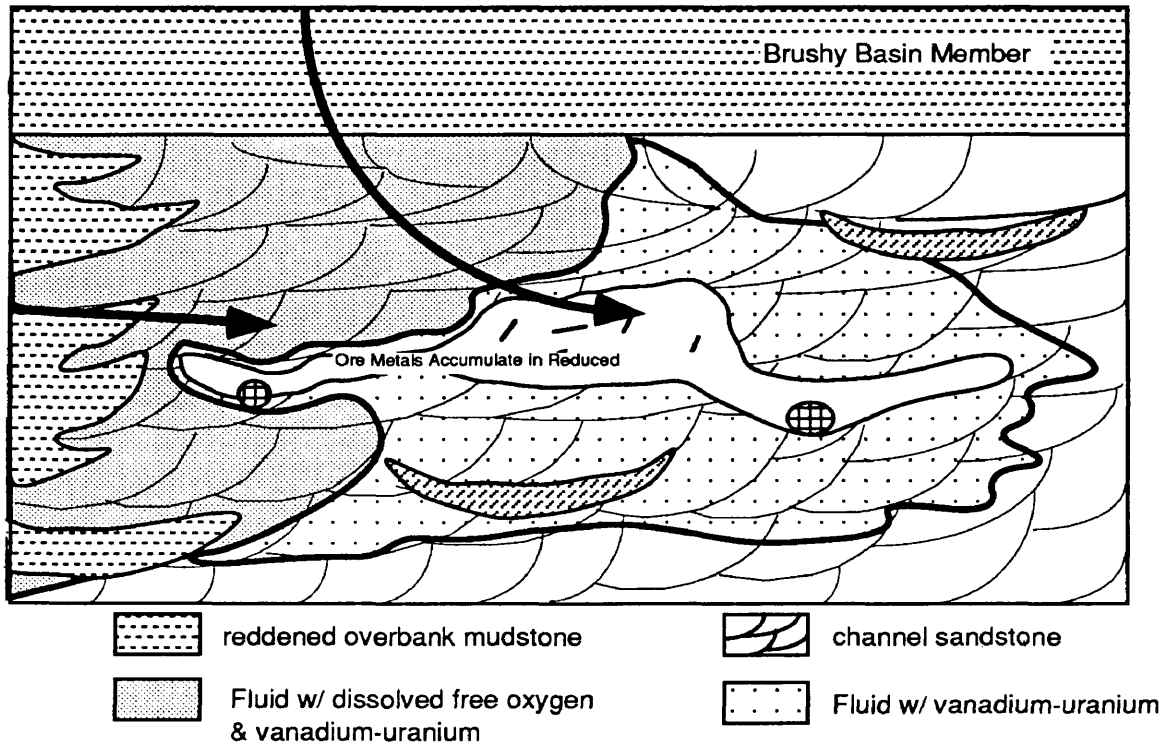


Figure 26b: Shallow Burial II Stage. Oxygenated meteoric water from the Brushy Basin Member and the Salt Wash Member overbank mudstones entered reduced sandstones. The meteoric water carried vanadium and uranium. Dissolved oxygen was depleted from iron (II) oxidation. Ore metals precipitated because of reduction during reaction with dissolved organic matter and H_2S .

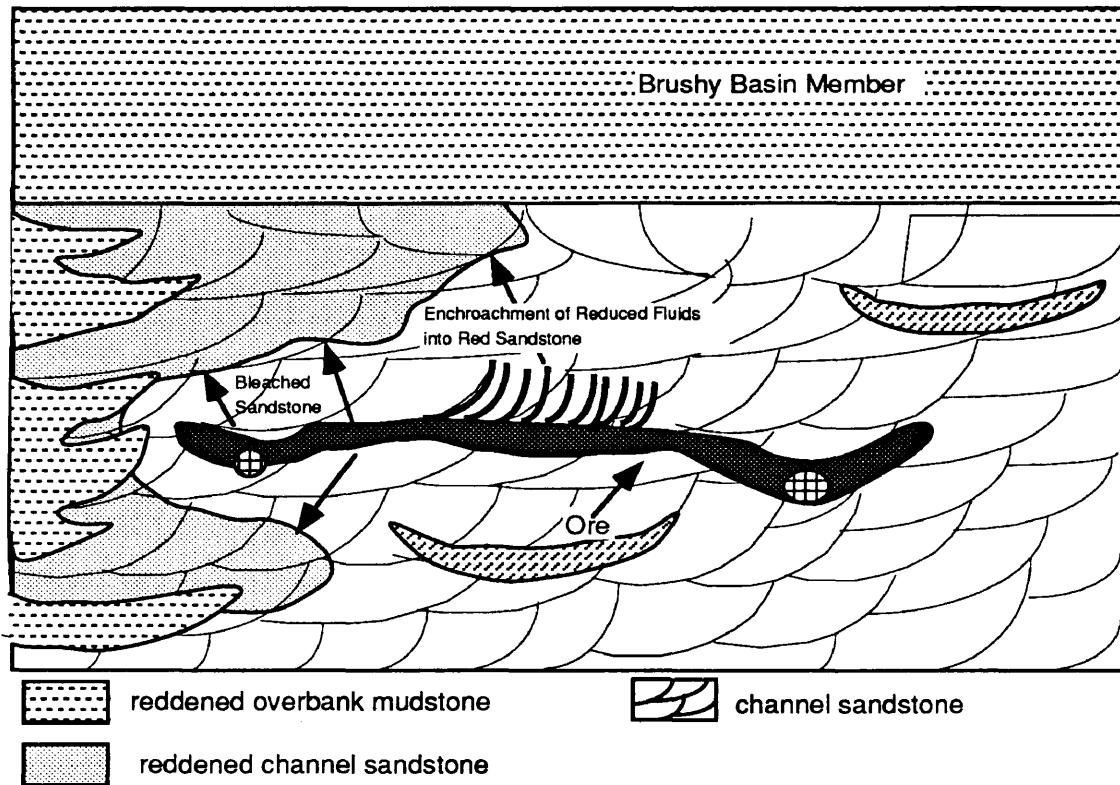


Figure 26c: Diagram summarizing the Deep Burial Stage. Arrows show the bleaching of reddened sandstone after flux of oxidizing fluid from the Brushy Basin Member stops, by dissolved organic matter and bacterial activity from reduced sandstone.

oxygenated water also formed goethite and hematite by oxidation of previously reduced rocks. Evidence for the introduction of an oxygenated fluid into a portion of reduced sandstone is the partial dissolution of pyrite and the preservation of detrital Fe-Ti oxides that were slightly altered by iron dissolution. Once the dissolved free oxygen was depleted, this fluid continued on the flow path until oxidized metals that it carried were reduced and precipitated. The oxygenated meteoric water is inferred to be weakly alkaline because these conditions favor transport of vanadium and uranium and magnetites and ilmenites were only partially altered.

After the Brushy Basin Member was deposited, the supply of oxygenated pore water ceased. When oxygen was no longer supplied to maintain the iron oxidizing conditions, the reducing pore-waters that were still being generated by dissolved organic matter and bacterial activity encroached into the oxidizing sandstone (Figure 26c). Iron oxides were partially dissolved and now are found only in low permeability zones, such as along cross-bedding laminae, under quartz overgrowths, and only within the cores of pore-filling clays. Hematized magnetites were also partially dissolved. Along with the production of pyrite, native sulfur precipitated during the reactions of H_2S with iron oxides. Microcrystalline TiO_2 may have formed by reaction of hematite with Ti(III) complexed with organic acids.

REFERENCES CITED

- Adams, S.S., 1991, Evolution of genetic concepts for principle types of sandstone uranium deposits in the United States: Economic Geology Monograph 8, p. 225-248.
- Adams, S.S., Curtis, H.S., and Hafen, P.L., 1974, Alteration of detrital magnetite-ilmenite in continental sandstones of the Morrison Formation, New Mexico, in Formation of uranium deposits: Vienna, International Atomic Energy Agency, p. 219-253.
- Adler, H. H., 1974, Concepts of uranium-ore formation in reducing environments in sandstones and other sediments, in Formation of uranium deposits: Vienna, International Atomic Energy Agency, p. 141-168.
- Austin, S.R., 1960, Ilmenite, Magnetite, and feldspar alteration under reducing conditions: Economic Geology, v. 55, p.1758-1759.
- Berner, R.A., 1970, Sedimentary pyrite formation: American Journal of Science, v. 268, p. 1-23.
- Birnbaum, S.J., and Wireman, J.W., 1984, Bacterial sulfate reduction and pH: implications for early diagenesis: Chemical Geology, vol. 43, p. 143-149.
- Boggs, S. Jr., 1987, Principles of sedimentology and stratigraphy, Columbus: Merrill Publishing Company, 784 p.

- Bowers, H.E., and Shawe, D.R., 1961, Heavy minerals as guides to uranium-vanadium ore deposits in the Slick Rock district, Colorado: U.S. Geological Survey Bulletin 1107-B, p. 168-218.
- Breit, G.N., 1986, Geochemical study of authigenic minerals in the Salt Wash Member of the Morrison Formation, Slick Rock district, San Miguel County, Colorado: Golden Colorado, Ph.D. thesis, Colorado School of Mines, 267 p.
- Breit, G.N. and Goldhaber, M.B., 1989, Hematite-enriched sandstones and chromium-rich clays - clues to the origin of vanadium-uranium deposits in the Morrison Formation, southwestern Colorado and southeastern Utah, USA *in* Uranium Resources and Geology of North America: Vienna, Austria, International Atomic Energy Agency, TECDOC-500, p. 201-226.
- Breit, G. N., Shawe, D. R., Simmons, E. C., 1990, Authigenic barite as an indicator of fluid movement through sandstones within the Colorado Plateau: *Journal of Sedimentary Petrology*, v. 60, p. 1-13.
- Cadigan, R.A., 1967, Petrology of the Morrison Formation in the Colorado Plateau region: U.S. Geological Survey Profession Paper 556, 113p.
- Carrol, D., 1960, Ilmenite alteration under reducing conditions in unconsolidated sediments: *Economic Geology*, v. 5, p. 618-619.

- Cater, F.W., 1970, Geology of the salt anticline region in southwestern Colorado: U.S. Geological Survey Professional Paper 637, 75 p.
- Fischer, R.P., and Hulpert, L.S., 1952, Geology of the Uravan mineral belt: U.S. Geological Survey Bulletin 988-A, p. 1-13.
- Flinter, B.H., 1959, The alteration of Malayan ilmenite grains and the question of "arizonite": *Economic Geology*, v. 54, p.720-729.
- Frankel, R.B. and Blakemore, R.P., 1984, Precipitation of Fe_3O_4 in magnetotactic bacteria: *Philosophical Transactions of the Royal Society of London, Series B*, vol. 304, p. 567-574.
- Gallagher, K.J., Feitknecht, W., and Mannweiler, U., 1968, Mechanism of oxidation of magnetite to gamma - Fe_2O_3 : *Nature*, v. 217, p. 1118-1121.
- Gardner, L.R., 1973, Chemical models for sulfate reduction in closed anaerobic marine environments: *Geochimica et Cosmochimica Acta*, vol. 37, p. 53-68.
- Garrels, R.M., Larsen, E.S., Pommer, A.M., and Coleman, R.G., 1959, Detailed chemical and mineralogical relations in two vanadium-uranium ores, in Garrels, R.M., and Larsen E.S., *Geochemistry and mineralogy of the Colorado Plateau uranium ores*: U.S. Geological Survey Professional Paper 320, p. 165-184.

- Goddard, E.N., Trask, P.D., De Ford, R.K., Rove, O.N., Singewald, J.T., and Overbeck, R.M., 1948, Rock-color chart (1979 ed.): Boulder, Colorado, Geological Society of America.
- Goldhaber, M.B., and Kaplan, I.R., 1974, The sedimentary sulfur cycle, in Goldberg, E.D., ed., *The sea*, v. 5: New York, John Wiley and Sons, p. 569-655.
- Granger, H.C., and Warren, C.G., 1979, The importance of dissolved free oxygen during formation of sandstone-type uranium deposits, U.S. Geological Survey Open-File Report 79-1603, 20 p.
- Gruner, J.W., 1959, The decomposition of ilmenite, *Economic Geology*, v. 54, p. 1315-1323.
- Hudson, R.J. and Morel, F.M., 1989, Distinguishing between extra- and intracellular Fe in marine phytoplankton: *Limnol. Oceanogr.*, v. 34, p. 1113-1120.
- Imlay, R.W., 1980 Jurassic paleobiogeography of the conterminous United States in its continental setting: U.S. Geological Survey Professional Paper 1062, 134 p.
- Jensen, M. L., 1958, Sulfur isotopes and the origin of sandstone type uranium deposits: *Economic Geology*, v. 53, p. 598-616.
- Langmuir, Donald, 1978, Uranium solution-mineral equilibria at low temperatures with applications to sedimentary ore deposits: *Geochimica et Cosmochimica Acta*, v. 42, p. 547-569.

- Lerman, A., 1988, Geochemical processes water and sediment environments, Robert E. Krieger Publishing Company: Malabar, Florida, 481 p.
- Lynd, L.E., 1961, Conditions for ilmenite alteration: *Economic Geology*, v. 56, p. 994-1000.
- McBride, E. F., 1989, Quartz cement in sandstones: A review: *Earth-Science Reviews*, v. 26, p. 69-112.
- Miller, D.N. and Folk, R.L., 1955, Occurrence of detrital magnetite and ilmenite in red sediments: New approach to significance of redbeds: *American Association of Petroleum Geologist*, v. 39, p. 338-345.
- Miller, D.S., and Kulp, J.L., 1963, Isotopic evidence on the origin of the Colorado Plateau uranium ores: *Geological Society of America Bulletin*, vol. 74, p. 609-630.
- Nestler, R.K., and Chenoweth, W.L., 1958, Geology of the uranium deposits of the Lukachukai Mountains, Apache County, Arizona: U.S. Atomic Energy Commission RME-118, 64 p.
- Northrop, H.R., 1982, Origin of the tabular-type vanadium-uranium deposits in the Henry structural basin, Utah: unpublished Ph.D. thesis, Colorado, School of Mines, 339 p.
- Northrop, H.R., Goldhaber, M.B., Landis, G.P., and Unruh, J.W., 1990, Part I. Geochemical and mineralogical evidence for the sources of the ore-forming fluids, in Northrop, H.R. and Goldhaber, M.B.,

Genesis of the tabular-type vanadium-uranium deposits of the Henry Basin, Utah: *Economic Geology*, v. 85, p. 215-236.

Peterson, F., and Turner-Peterson, C.E., 1980, Lacustrine-humate model: Sedimentological and geochemical model for tabular sandstone uranium deposits in the Morrison Formation, Utah, and application to uranium exploration: U.S. Geological Survey Open-File Report 30-319, 40 p.

Postgate, J.R., F.R.S, Kelly, D.P., ed, 1982, Sulphur Bacteria: *Phil. Transactions of the Royal Society of London*, B 298, p. 429-602.

Pye, K., 1983, Red beds in Goudie, A. S., and Pye, K., eds, *Chemical sediments and geomorphology: precipitates and residua in the near-surface environment*: New York: Academic Press, p. 227-263.

Rickard, D.T., 1974, Kinetics and mechanism of the sulfidation of goethite: *American Journal of Science*, v. 274, p. 941-952.

Ryan, J.N. and Gschwend, P.M., 1991, Extraction of iron oxides from sediments using reductive dissolution by titanium(III): *Clay and Clay Minerals*, v. 39, no. 5, p. 509-518.

Saucier, A.E., 1980, Tertiary oxidation in the Westwater Canyon Member of the Morrison Formation, in, Rautman, C. A., comp., *Geology and mineral technology of the Grants uranium region 1979*: New Mexico Bureau of Mines and Mineral Resources Memoir 38, p. 116-121.

- Shawe, D.R., 1968, Petrography of sedimentary rocks in the Slick Rock district, San Miguel and Dolores Counties, Colorado: U.S. Geological Survey Professional Paper 576-B, 34 p.
- Shawe, D.R., 1976, Sedimentary rock alteration in the Slick Rock district, San Miguel and Dolores Counties, Colorado: U.S. Geological Survey Professional Paper 576-D, 51 p.
- Shawe, D.R., Simmons, G.C., Archbold, N.L., 1968, Stratigraphy of Slick Rock district and vicinity, San Miguel and Dolores Counties, Colorado: U.S. Geological Survey Professional Paper 576-A, 108p.
- Smith, D.B., Zielinski, R.A., and Rose, W.I., 1982, Leachability of uranium and other elements from freshly erupted volcanic ash: *Journal of Volcanology and Geothermal Research*, v. 13, p. 1-30.
- Stanton, M.R. and Goldhaber, M.B., 1991, An experimental Study of goethite sulfidization - relationships to the Diagenesis of iron and sulfur: U.S. Geological Survey Bulletin 1978.
- Stumm, W., and Morgan, J. J., 1981, *Aquatic chemistry*, 2nd ed. New York: Wiley-Interscience.
- Thamm, J.K., Kovschak, A.A., and Adams, S.S., 1981, Geology and recognition criteria for sandstone uranium deposits of the Salt Wash type, Colorado Plateau Province: U.S. Department of Energy GJBX-6(81), 135 p.

- Torrent, J. and Schwertmann, U., 1986, Influence of hematite on the color of red beds: *Journal of Sedimentary Petrology*, vol. 57, p. 682 - 686.
- Tyler, Noel, and Ethridge, F.G. 1983, Depositional setting of the Salt Wash Member of the Morrison Formation: *Journal of Sedimentary Petrology*, v. 53, p. 67-82.
- Walker, T.W., 1976, Diagenetic origin of continental red beds, in *The continental Permian in central, west, and south Europe, proceedings of the NATO advanced study institute, Mainz, Germany, 1974*, edited by Falke, H., D.Reidel, Hingham, Mass., p. 240-282.
- Whitney, C. G., and Northrop, H.R., 1986, Vanadium chlorite from a sandstone-hosted vanadium-uranium deposit, Henry basin, Utah: *Clays and Clay Minerals*, v. 34, p. 488-495.

APPENDIX

Sample number	Color	Matrix Supported	Volume % Epoxy	Chert & Chalcedony	Calcite	Gypsum	Magnetite & Ilmenite	Leucoxene	Pyrite	Native Sulfur	Hematite between Quartz Grains & overgrowths	Hematite w/ in pore-filling Qtz	Pore-filling Hematite	Hematite w/ in Calcite	Hematized Magnetite	Hematite Stained Clay	Hematite Stained Leucoxene	Hematite inclusion in Leucoxene	Hematite in Rock Fragments
S1R	5R 4/2	clay, calcite	0	M	Poik	n	tr	M	M	n	n	n	n	M	n	n	M	n	M
S4mG	5GY9/1	n	10	tr	Pore	n	tr	M	M	n	n	tr	n	tr	tr	n	tr	n	tr
S7mG	5GY 9/1	n	10	M	Pore	n	tr	M	n	n	n	tr	n	tr	n	n	tr	n	tr
S10mG	5Y 8/1	n	10	M	Pore	n	n	M	n	n	n	tr	n	tr	M	n	tr	n	tr
S12mG	5YR 8/1	n	10	M	Pore	n	M	M	n	n	n	tr	n	tr	M	n	M	n	tr
S15mR	5R 8/1.5	n	0	M	Pore	n	M	M	n	n	tr	M	n	M	M	n	M	n	M
S17mR	5R 7/2	n	tr	M	Pore	M	M	M	tr	n	M	M	n	M	M	n	M	n	M
S19mR	10R 7/2	n	tr	M	Pore	M	M	M	n	n	M	M	tr	M	M	M	M	tr	M
S21mR	5R 6/2	clay	tr	M	Pore	M	M	M	n	n	ab	M	M	M	M	M	Ab	M	M
S23mR	5R 6/2	n	tr	M	Pore	n	M	M	n	M	ab	Ab	Ab	M	M	M	Ab	M	M
S25mR	10R 6/2	n	0	M	Pore	n	M	M	n	n	M	M	M	M	M	M	M	M	M
S28mR	10R 5/2	n	10	M	Pore	n	tr	M	n	n	L	M	tr	M	M	M	M	n	M
S29mG	5Y 6/1	n	10	M	Poik&Pore	n	tr	M	M	n	tr	M	n	n	M	n	M	n	M
HRM1R	10R 6.5/3	n	20	M	Pore	n	tr	M	tr	n	tr	tr	n	n	M	n	M	n	M
HRM3R	10R 6/2	n	10	M	Pore	n	tr	M	tr	n	tr	tr	n	n	M	n	n	n	n
HRM4R	9R 7/4	n	20	M	Pore	n	tr	M	n	n	tr	tr	M	M	M	M	M	n	M
HRM5R	10R 7.5/4	n	10	M	Pore	n	M	M	tr	n	tr	n	n	n	M	n	n	n	n
HRM6R	7R 7.5/4	n	20	M	Pore	n	tr	M	tr	n	tr	n	n	n	M	M	M	M	M
D26G	5YR 3/1	clay	10	M	Pore	n	tr	M	n	n	tr	tr	n	n	M	M	M	n	M
D17R	5R 7/2	clay	20	M	Pore	n	M	M	n	n	M	M	n	n	M	Ab	M	n	M
D10R	5YR 8/1	calcite	10	M	Poik	n	M	M	tr	n	tr	M	M	M	M	Ab	M	n	M
DV-120R	10R 6/2	n	0	M	Pore	n	M	M	n	n	M	M	n	M	M	M	M	n	M

R - Red
 G - Green
 S - Sunday Mine Samples
 D - Deremo Mine Samples
 HRM - Horse Range Mesa Samples
 DV-120 - Atomic Energy Core Samples

m - meters for Sunday Mine Samples
 n - none detected
 tr - trace mount detected
 M - moderate amount
 Ab - abundant amount

